Thermal model: a brief introduction and applications

J. Billard
Institut de Physique Nucléaire de Lyon / CNRS / Université Lyon 1

DRTBT
Aussois, March 28, 2024

Outline of this lecture

Part I: Basics of electro-thermal modelling

Part II: Illustration with Ricochet detectors

Part III: Other recent examples:

- *High impedance TES X-ray calorimeter*
- *Dark matter DC heating*

Conclusion

Part I: Basics of electro-thermal modelling

$$\Delta T = \frac{E}{C}$$

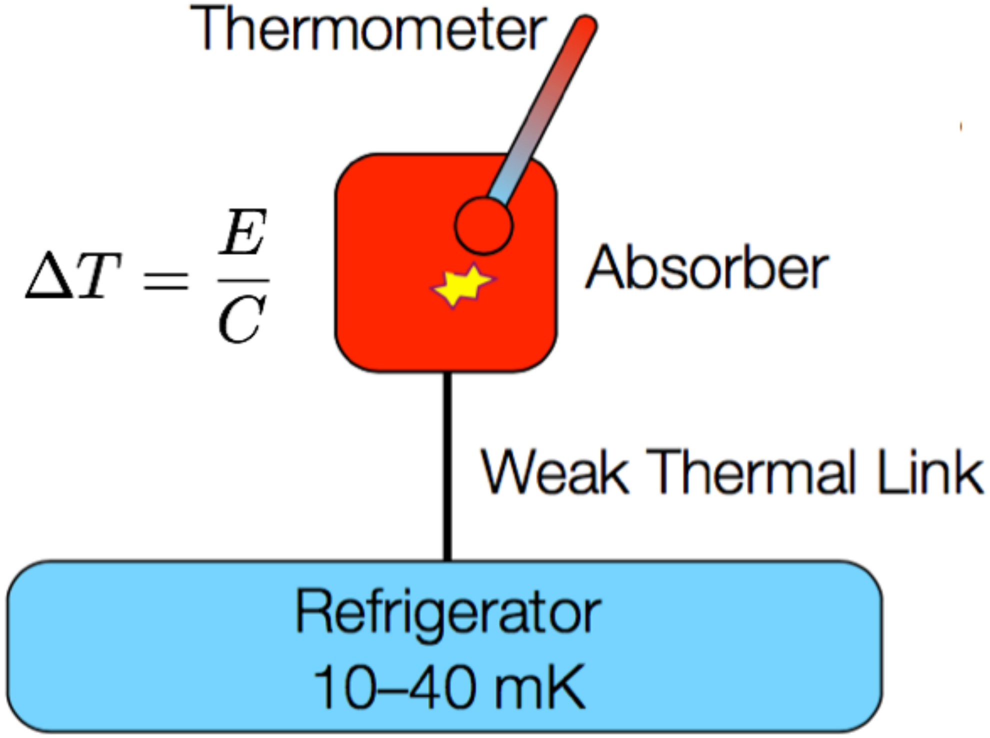

- **Based on:**
  - K. D. Irwin and G. C. Hilton, Transition-Edge Sensor, In : Cryogenic Particle Detection. Ed by C. Enss. Berlin : Springer, 2005. Chap 3, pp. 63-149.
  - D. McCamon, Thermal Equilibrium Calorimeters – An Introduction, In : Cryogenic Particle Detection. Ed by C. Enss. Berlin : Springer, 2005. Chap 3, pp. 63-149.
  - M. Lindeman, Ph.D. thesis, University of California at Davis, (2000)

Part I: Basics of electro-thermal modelling

$$\Delta T = \frac{E}{C}$$

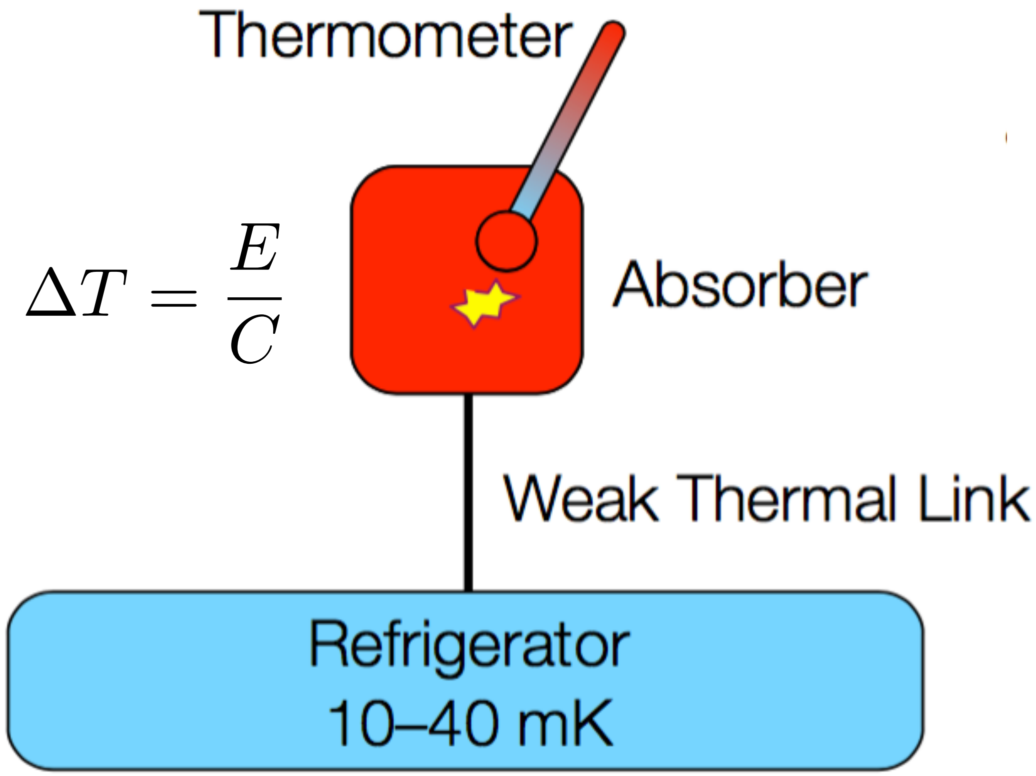

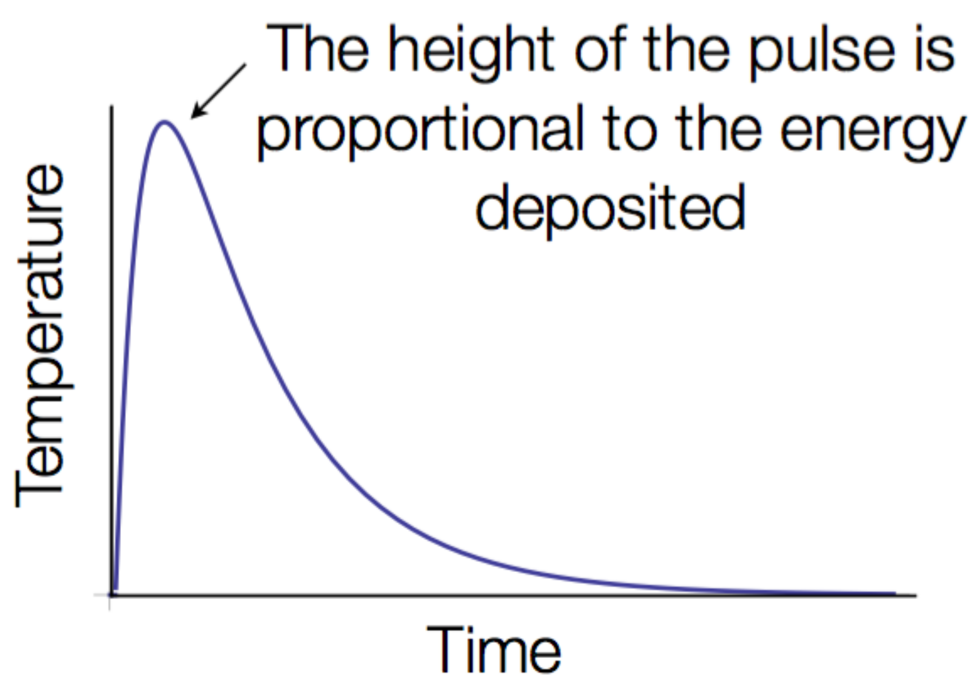

- Advantages of a phonon readout:
  - Direct measurement of the recoil energy, *no quenching involved*
  - ~100 % of the recoil energy is sensed, *allowing for low-thresholds*
  - *No intrinsic threshold*
  - From thermodynamics, ultimate energy resolution is: **~eV (RMS) for ~ 10 g detectors**
- Commonly used phonon readouts
  - High impedance NTD
  - High impedance TES
  - Low-impedance TES

$$E_T \propto M^n_{\mathrm{detector}}$$

Scaling law (n~1) depends on phonon readout

Part I: Basics of electro-thermal modelling

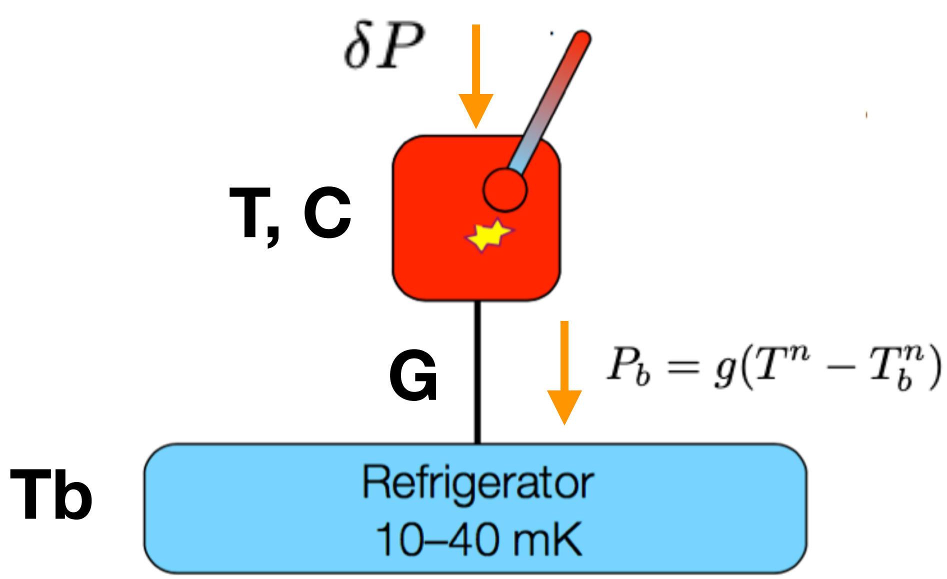

We can derive the usual thermal equation with no Joule heating:

$$C\frac{dT}{dt} = -P_b + \delta P$$

Using first order perturbation: $T(t) \approx \bar{T} + \delta T(t)$

$$\begin{aligned} C\frac{d\Delta T}{dt} &= -ng\bar{T}^{n-1}\Delta T + \delta P \\ &= -G\Delta T + \delta T \end{aligned}$$

Laplace transform

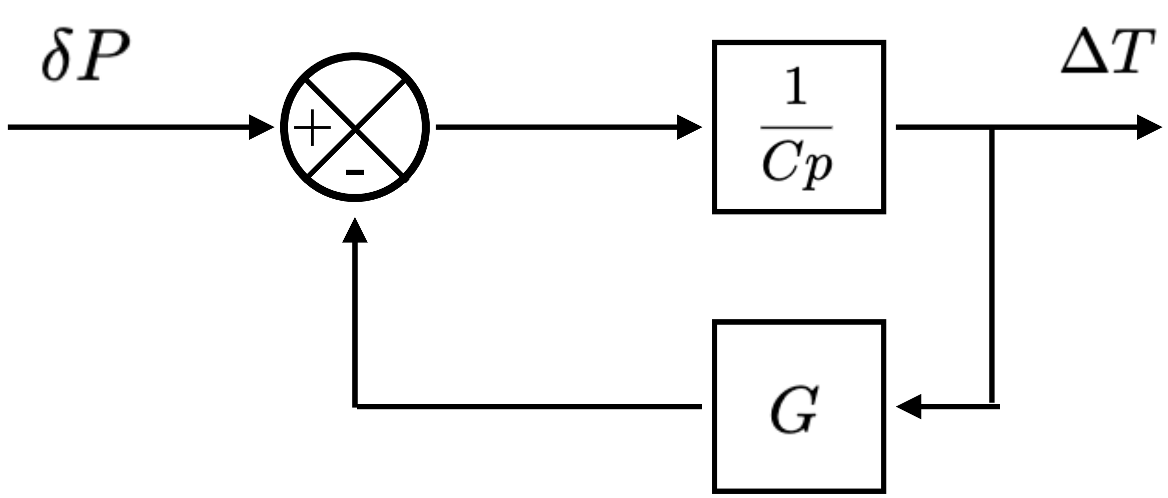

$$Cp\Delta T = -G\Delta T + \delta P$$

$$\Delta T = \delta P \frac{1}{Cp + G}$$

$$\Delta T(\omega) = \delta P(\omega)\frac{1}{C}\frac{\tau}{(1 + i\omega\tau)}, \text{ with } \tau = C/G$$

Part I: Basics of electro-thermal modelling

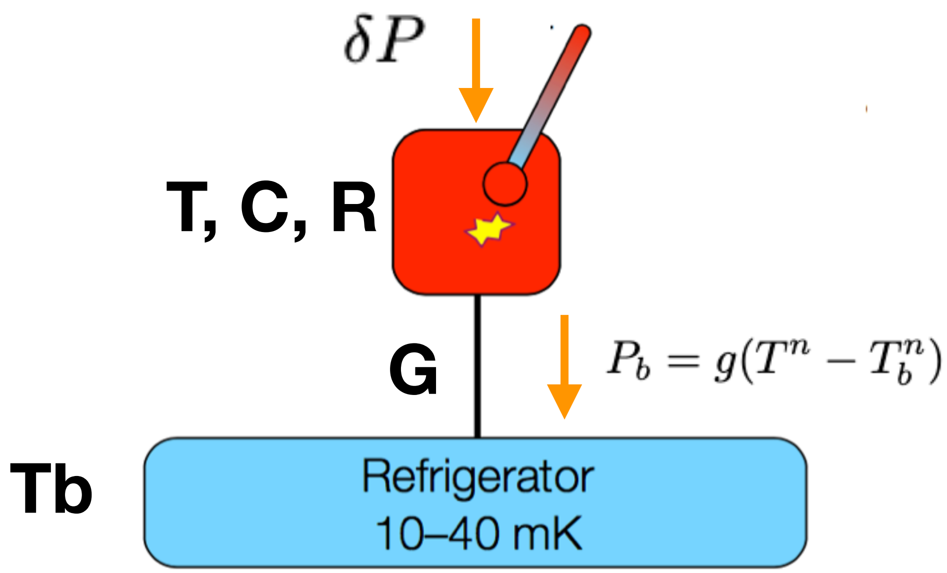

Electrical circuit to read the thermometer

(still with no Joule effect for now)

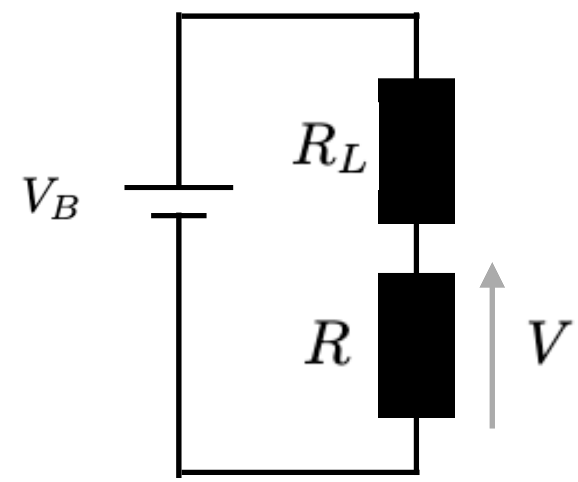

$$V = V_B \frac{R}{R_L + R}$$

1st order

$$\Delta V = \frac{\bar{V}}{\bar{R}} \frac{R_L}{R_L + \bar{R}} \left. \frac{dR}{dT} \right|_{\bar{T}} \Delta T$$

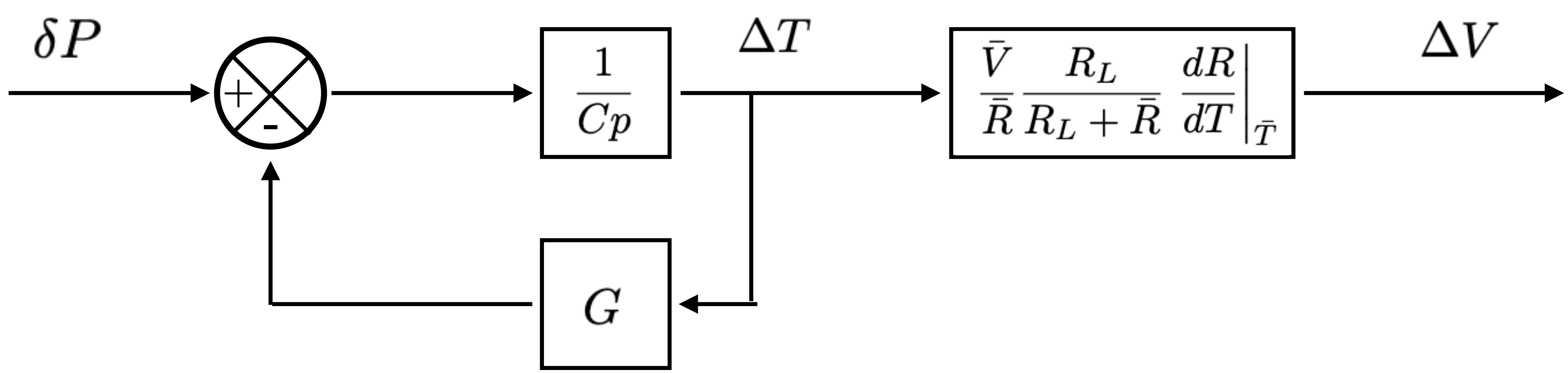

$$\Delta V(\omega) = \delta P(\omega) \frac{\bar{V}}{\bar{R}} \frac{R_L}{R_L + \bar{R}} \left. \frac{dR}{dT} \right|_{\bar{T}} \frac{\tau}{C} \frac{1}{(1 + i\omega\tau)}$$

(V/W)

Part I: Basics of electro-thermal modelling

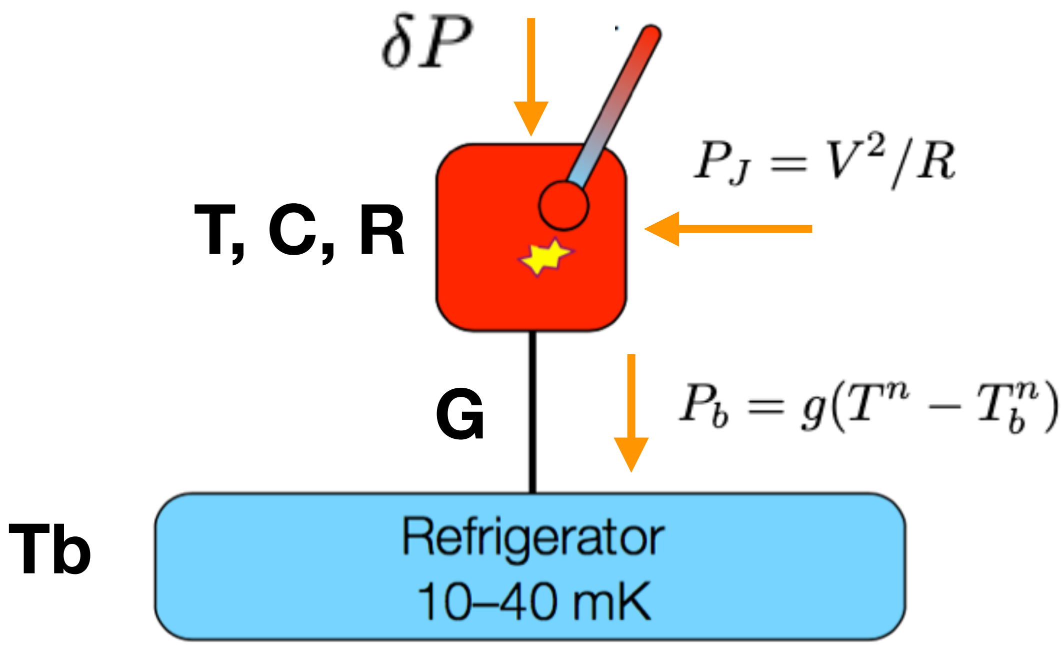

Now adding the Joule heating:

$$C\frac{dT}{dt} = -P_b + P_j + \delta P \qquad V = V_B\frac{R}{R_L + R}$$

$$C\frac{d\Delta T}{dt} = -G\Delta T + 2\frac{\bar{V}}{\bar{R}}\Delta V - \frac{\bar{V}^2}{\bar{R}^2}\left.\frac{dR}{dT}\right|_{\bar{T}}\Delta T + \delta P$$

$$\Delta V = \frac{\bar{V}}{\bar{R}}\frac{R_L}{R_L + \bar{R}}\left.\frac{dR}{dT}\right|_{\bar{T}}\Delta T$$

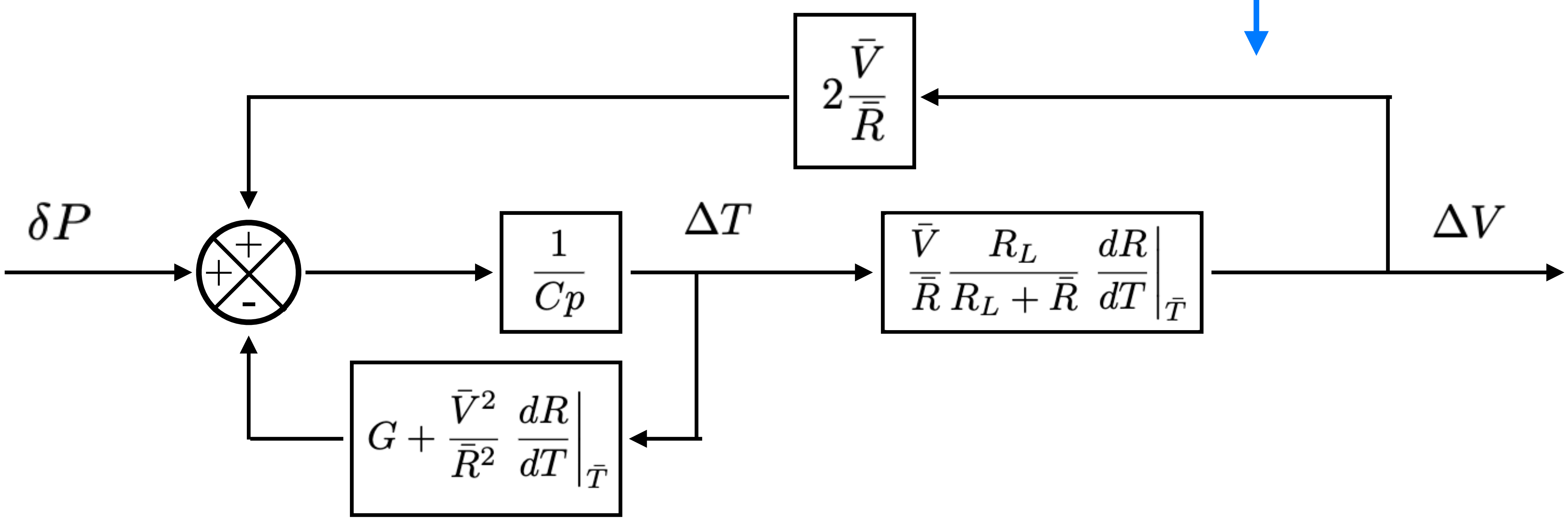

Part I: Basics of electro-thermal modelling

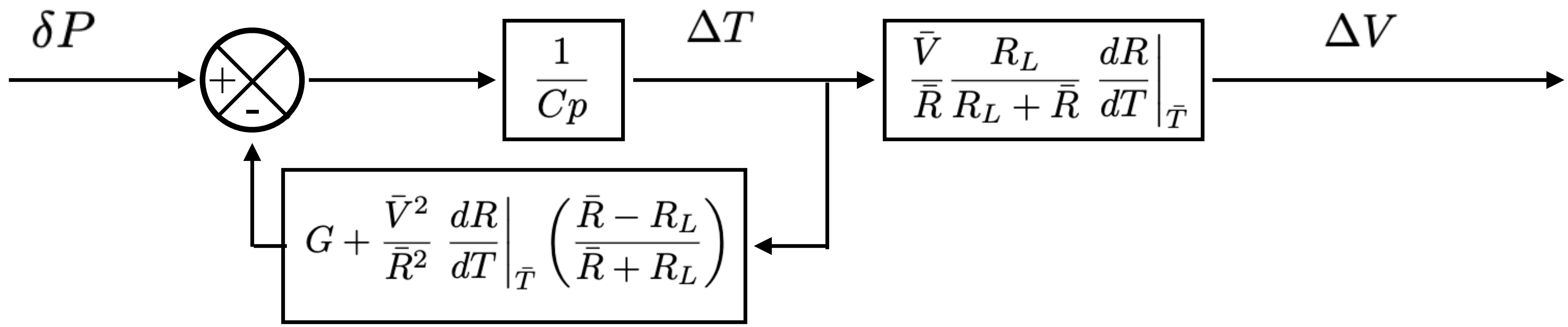

$$\Delta V(\omega) = \delta P(\omega) \frac{\bar{V}}{\bar{R}} \frac{R_L}{R_L + \bar{R}} \left.\frac{dR}{dT}\right|_{\bar{T}} \frac{1}{(1 + i\omega\tau')} \frac{\tau'}{C}$$ **(V/W)**

Similar equation as before with a modified time constant: $\tau' = C / \left[G + \frac{\bar{V}^2}{\bar{R}^2} \left.\frac{dR}{dT}\right|_{\bar{T}} \left(\frac{\bar{R} - R_L}{\bar{R} + R_L}\right) \right]$

$$\tau' = C/(G + G_{\mathrm{ETF}}) \quad \text{if} \quad R_L \gg R \quad \text{with} \quad G_{\mathrm{ETF}} = -\frac{\bar{V}^2}{\bar{R}^2} \left.\frac{dR}{dT}\right|_{\bar{T}}$$ *Negative ETF*

$$\tau' = C/G \quad \text{if} \quad R_L = R$$ *No ETF*

$$\tau' = C/(G - G_{\mathrm{ETF}}) \quad \text{if} \quad R_L \ll R$$ *Positive ETF*

Part I: Basics of electro-thermal modelling

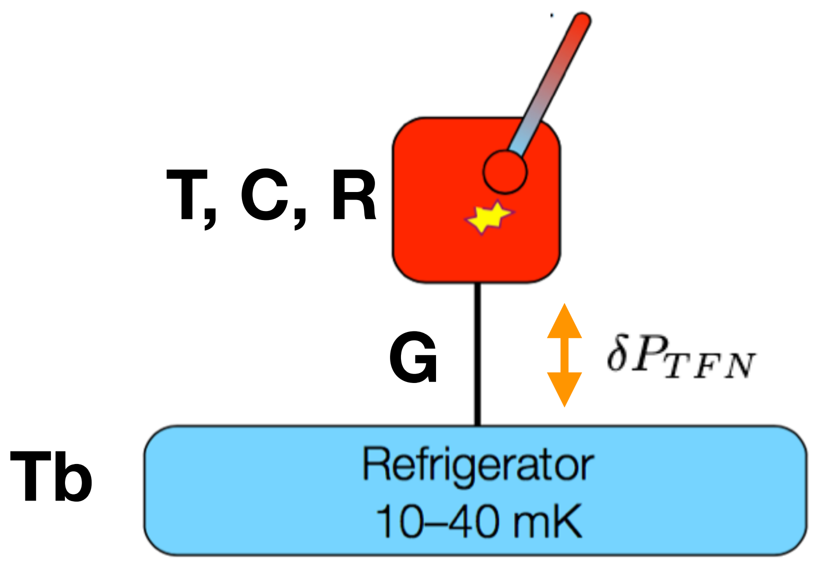

Fluctuations of the energy content in C due to exchanges via G is given by: $\langle \Delta E^2 \rangle = k_B T^2 C$

One can derive that to obtain such energy dispersion, the thermal fluctuation noise can be modelled as a white noise power spectrum:

$$\delta P_{TFN}^2(\omega) = 4k_B T_b^2 G_b \times F_{\rm link}(T, T_b, n) \qquad {\rm W^2/Hz}$$

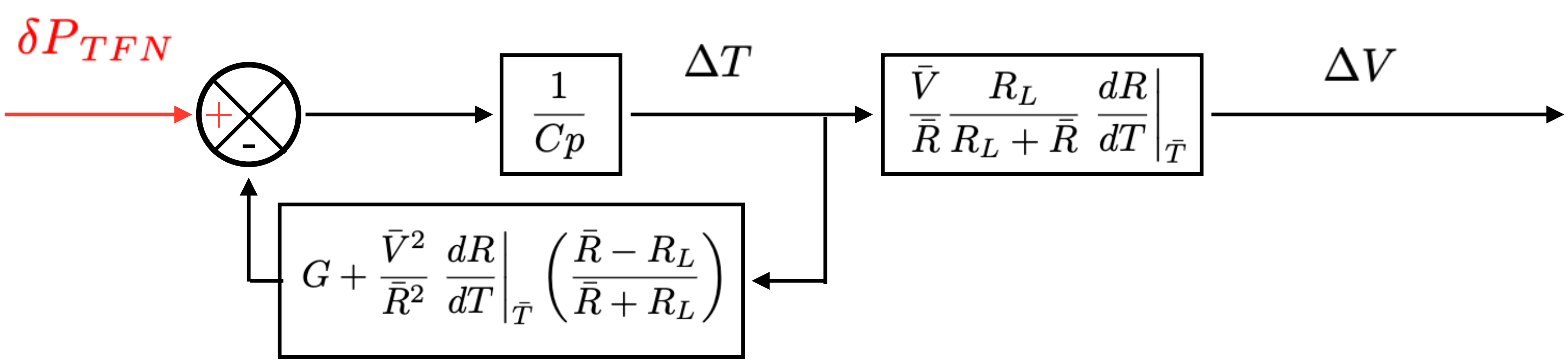

$$e_{TFN}(\omega) = \delta P_{TFN} \Delta V(\omega) = \delta P_{TFN} \frac{\bar{V}}{\bar{R}} \frac{R_L}{R_L + \bar{R}} \frac{dR}{dT}\Big|_{\bar{T}} \frac{1}{(1 + i\omega\tau')} \frac{\tau'}{C} \qquad ({\rm V}/\sqrt{\rm Hz})$$

*TFN noise is **unavoidable** and has similar frequency dependence as the signal — **ultimate noise***

Part I: Basics of electro-thermal modelling

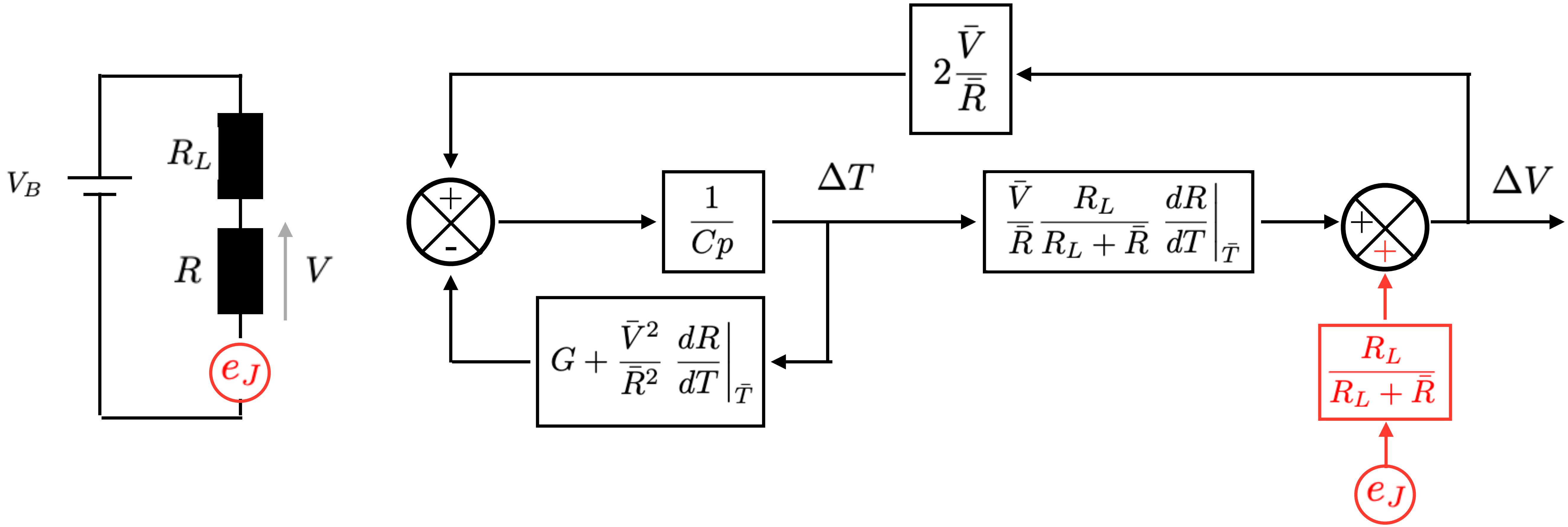

$$e_{n_J}(\omega) = \sqrt{4k_B\bar{T}\bar{R}}\frac{R_L}{R_L+\bar{R}}\left[1-\frac{2\bar{V}}{\bar{R}}\left(\frac{R_L}{R_L+\bar{R}}\right)\left.\frac{dR}{dT}\right|_{\bar{T}}\frac{1}{1+i\omega\tau''}\frac{\tau''}{G''}\right]^{-1} \quad \left(\mathrm{V}/\sqrt{\mathrm{Hz}}\right)$$

Assuming a current biased NTD:

$$R_L \gg \bar{R} \text{ and } \left.\frac{dR}{dT}\right|_{\bar{T}} < 0 \rightarrow$$

$$\lim_{\omega\to+\infty} e_{n_J}(\omega) = \sqrt{4k_B\bar{T}\bar{R}}$$ *Expected Johnson noise at high F*

$$\lim_{\omega\to 0} e_{n_J}(\omega) < \sqrt{4k_B\bar{T}\bar{R}}$$ *ETF damping at low F*

Note for a current biased high impedance TES, noise is boosted at low F !

Part II: Illustration with Ricochet detectors

Ricochet coll., Eur. Phys. J. C **84** (2024), 186

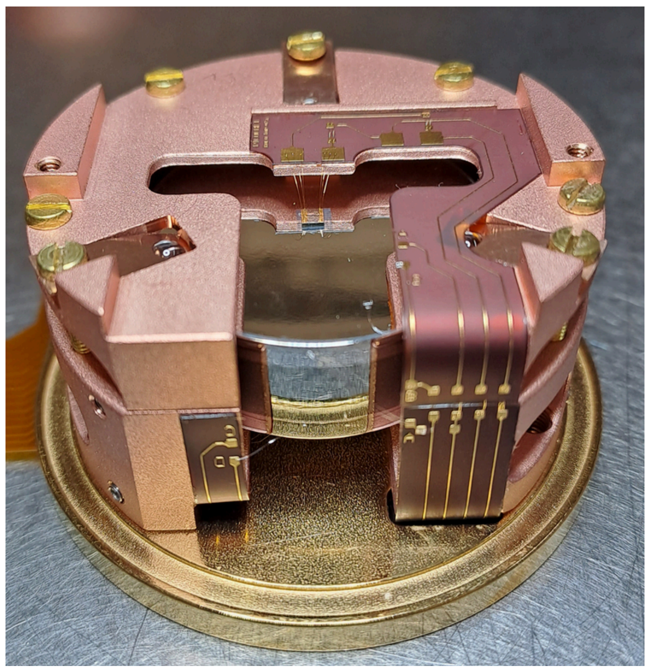

Detector: 42 g Ge

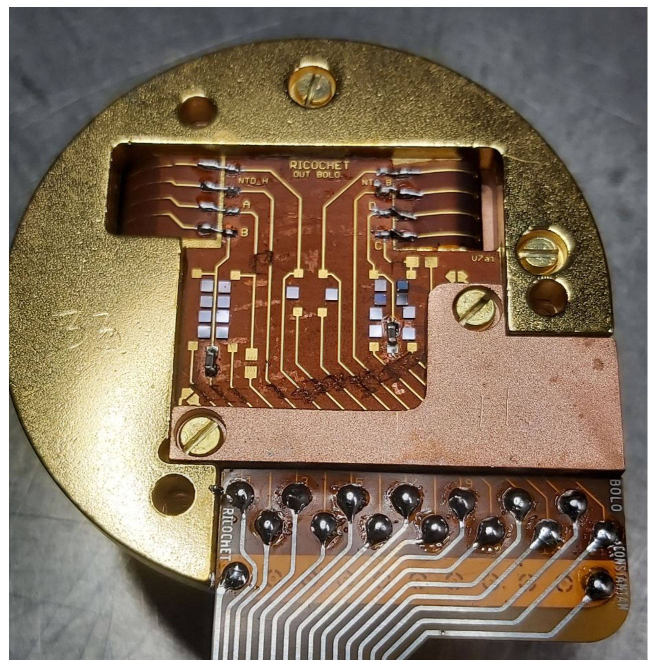

10 mK electronics

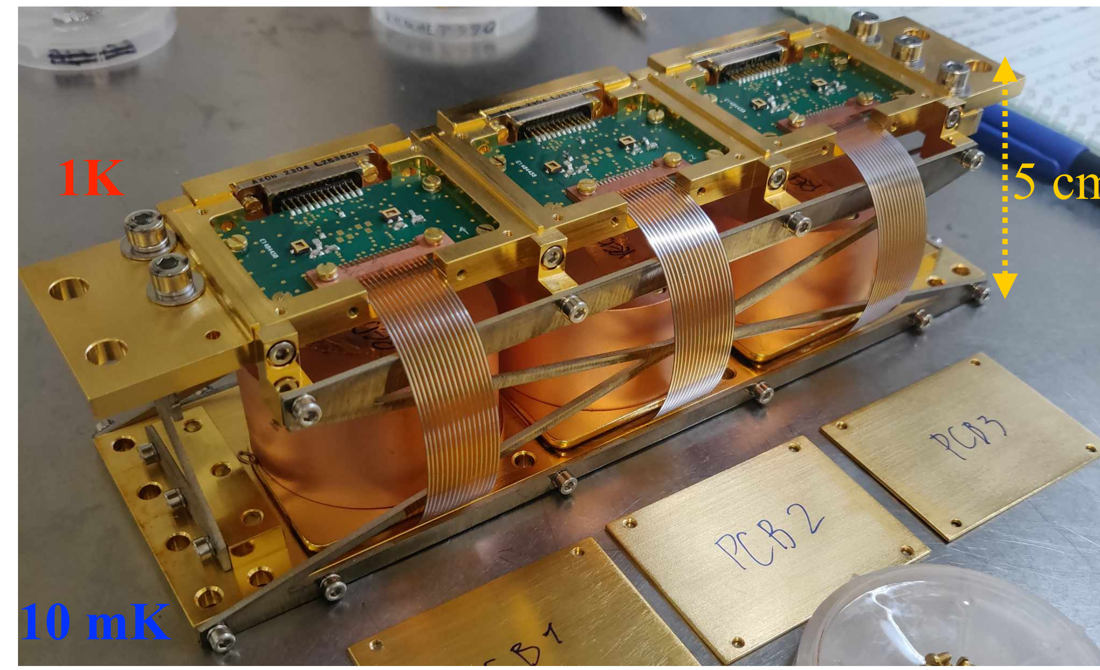

1K-10mK CryoCube integration

- **Measurement of both heat and ionisation**
- Spin off, or upgrade from the EDELWEISS-III experiment/technology:
  - Must accommodate the migration from wet cryostat to dry cryostat (and the ILL environment)
  - Must accommodate for above ground operation
- Targeted performance: **10 eV (RMS) heat** and 20 eVee (RMS) ionisation

Part II: Illustration with Ricochet detectors

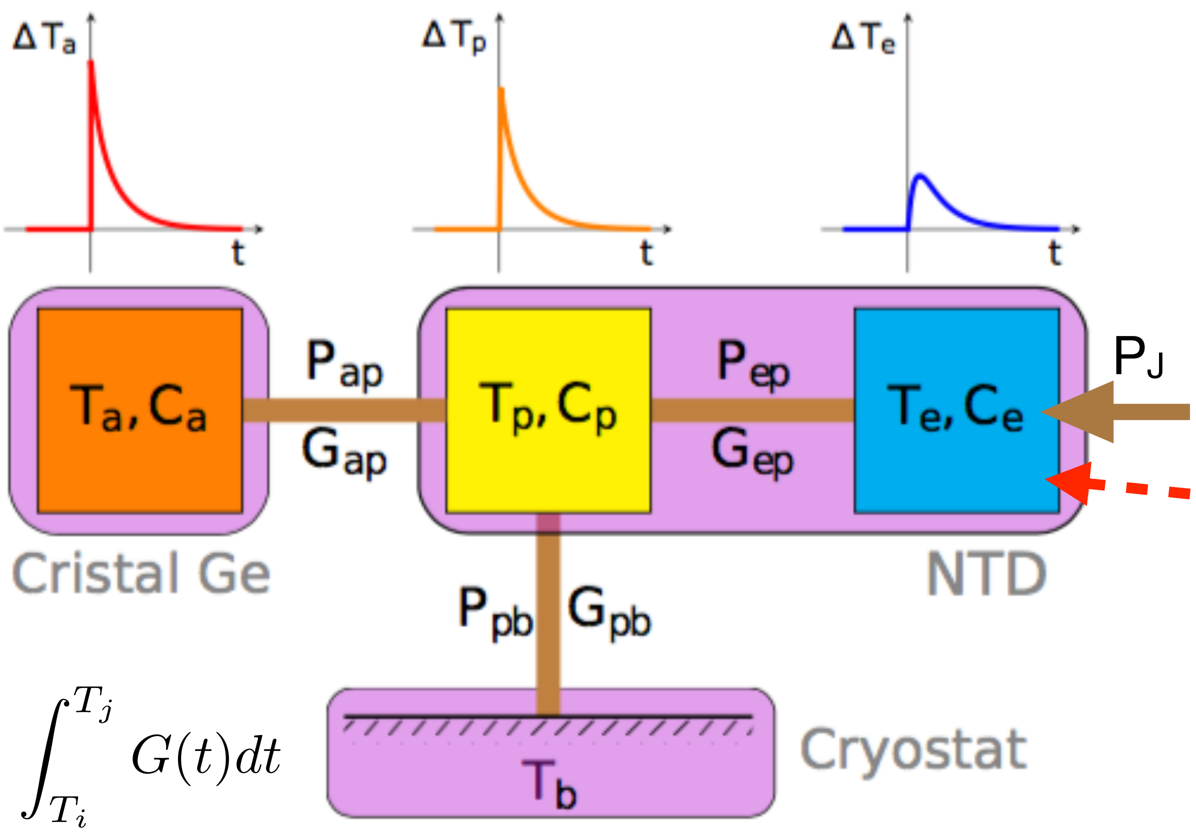

$$P_{ij} = \int_{T_i}^{T_j} G(t)dt$$

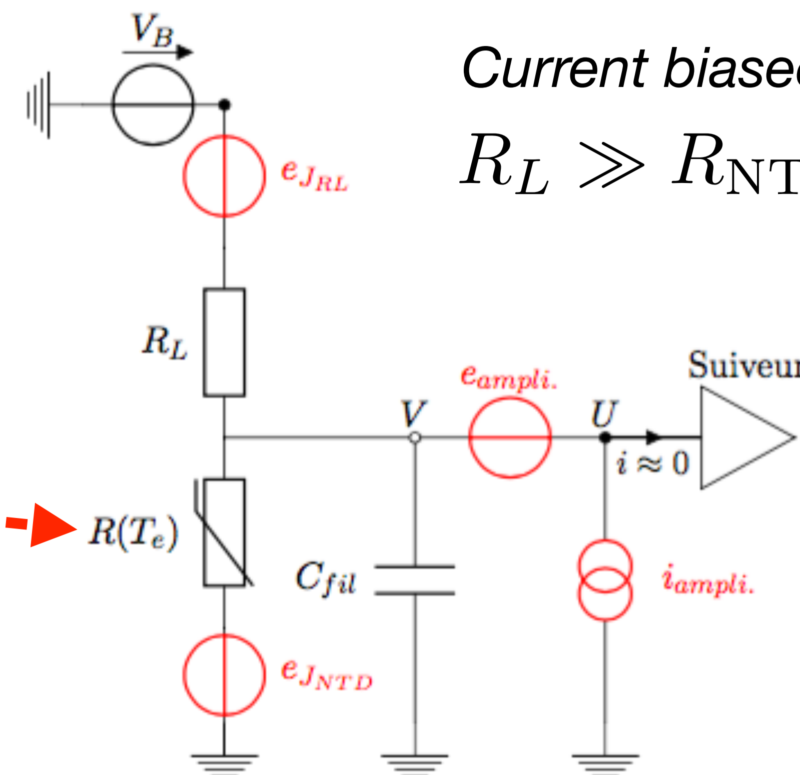

Current biased:

$$R_L \gg R_{\mathrm{NTD}}$$

Electro-thermal model:

$$R_0 = 1.04 \pm 0.02 \ [\Omega]$$
$$T_0 = 4.77 \pm 0.01 \ [\mathrm{K}]$$
$$g_{ep} = 55.6 \pm 0.5 \ [\mathrm{W/K^6/cm^3}]$$
$$g_k = (5.12 \pm 0.03) \times 10^{-5} \ [\mathrm{W/K^4/mm^2}]$$
$$g_{glue} = (1.46^{+1.75}_{-0.57}) \times 10^{-4} \ [\mathrm{W/K^{3.5}/mm^2}]$$
$$C_e = (1.03 \pm 0.04) \times 10^{-6} \times \bar{T}_e \ [\mathrm{J/K/cm^3}]$$
$$C_p = (2.66 \pm 0.05) \times 10^{-6} \times \bar{T}_p^3 \ [\mathrm{J/K/cm^3}]$$

$$C_a \frac{dT_a}{dt} = g_{glue} S_{NTD} \left(T_p^{n_g} - T_a^{n_g}\right)$$
$$C_p \frac{dT_p}{dt} = -g_{glue} S_{NTD} \left(T_p^{n_g} - T_a^{n_g}\right) + V_S g_{ep} \left(T_e^n - T_p^n\right) - g_k S_{Au} \left(T_p^{n_k} - T_b^{n_k}\right)$$
$$C_e \frac{dT_e}{dt} = \frac{V^2}{R(T_e)} - V_S g_{ep} \left(T_e^n - T_p^n\right)$$
$$C_{fil} \frac{dV}{dt} = \frac{V_B - V}{R_L} - \frac{V}{R(T_e)}$$

Based on D. Misiak, PhD

Part II: Illustration with Ricochet detectors

$$
\begin{aligned}
C_a \frac{dT_a}{dt} &= g_{glue} S_{NTD} \left(T_p^{n_g} - T_a^{n_g}\right) \\
C_p \frac{dT_p}{dt} &= -g_{glue} S_{NTD} \left(T_p^{n_g} - T_a^{n_g}\right) + V_S g_{ep} \left(T_e^{n} - T_p^{n}\right) - g_k S_{Au} \left(T_p^{n_k} - T_b^{n_k}\right) \\
C_e \frac{dT_e}{dt} &= \frac{V^2}{R(T_e)} - V_S g_{ep} \left(T_e^{n} - T_p^{n}\right) \\
C_{fil} \frac{dV}{dt} &= \frac{V_B - V}{R_L} - \frac{V}{R(T_e)}
\end{aligned}
$$

- Such set of coupled non-linear differential equation can be solved numerically
  - *Use of the **odeint** function in PYTHON for instance or pseudo-analytical model: M. Pedretti (PhD, CUORE)*
  - *Particularly relevant for high energy deposition (e.g. double beta experiments)*
- Or it can be solved analytically using first order perturbation theory
  - *Use of linear algebra*
  - *Particularly relevant for small energy deposition (low-threshold dark matter experiments)*

Steady state — Time evolution

$$
\begin{aligned}
T_a(t) &\approx \bar{T}_a + \delta T_a(t) \\
T_p(t) &\approx \bar{T}_p + \delta T_p(t) \\
T_e(t) &\approx \bar{T}_e + \delta T_e(t) \\
V(t) &\approx \bar{V} + \delta V(t)
\end{aligned}
$$

Part II: Illustration with Ricochet detectors

1st order perturbation around equilibrium:
- *Steady state solution*

No trivial solution
Has to be solved numerically

$$0 = g_{glue} S_{NTD} \left(\bar{T}_p^{n_g} - \bar{T}_a^{n_g} \right)$$

$$0 = -g_{glue} S_{NTD} \left(\bar{T}_p^{n_g} - \bar{T}_a^{n_g} \right) + V_S g_{ep} \left(\bar{T}_e^{n} - \bar{T}_p^{n} \right) - g_k S_{Au} \left(\bar{T}_p^{n_k} - \bar{T}_b^{n_k} \right)$$

$$0 = \frac{V^2}{R(\bar{T}_e)} - V_S g_{ep} \left(\bar{T}_e^{n} - \bar{T}_p^{n} \right)$$

$$0 = \frac{V_B - V}{R_L} - \frac{V}{R(\bar{T}_e)}$$

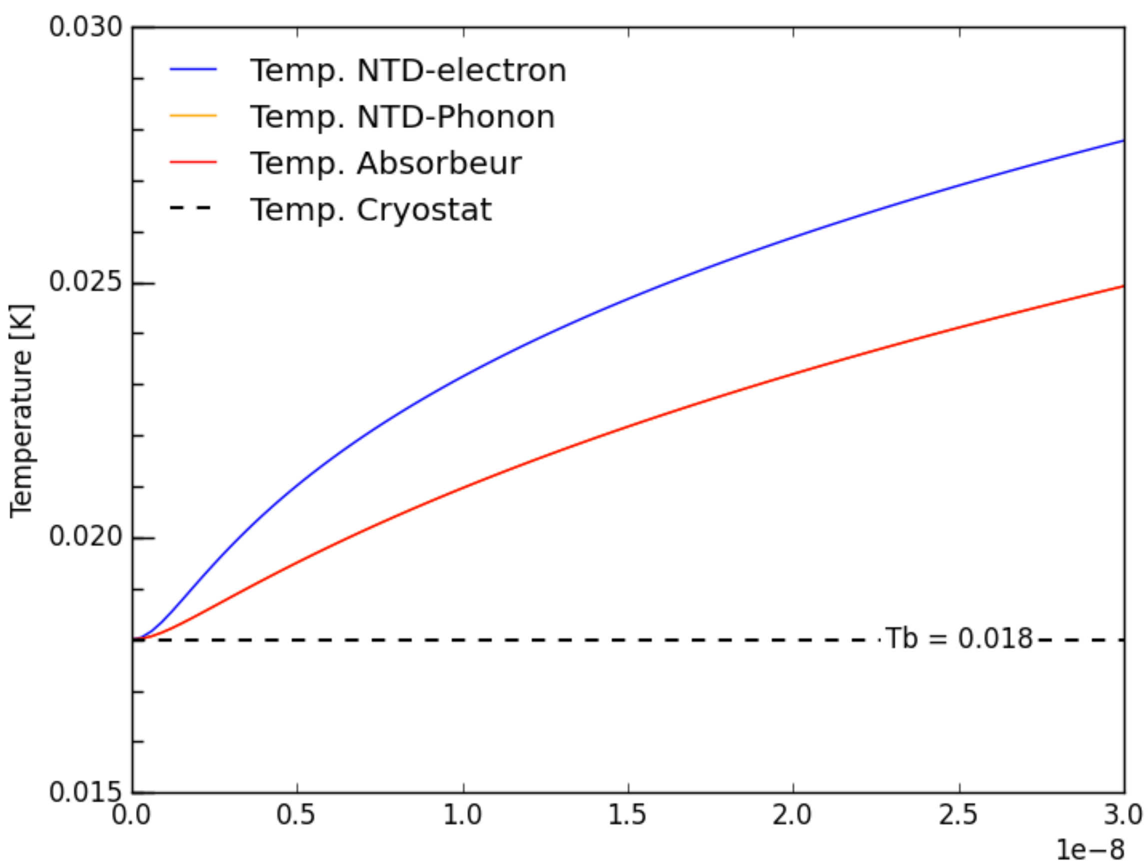

current [A]

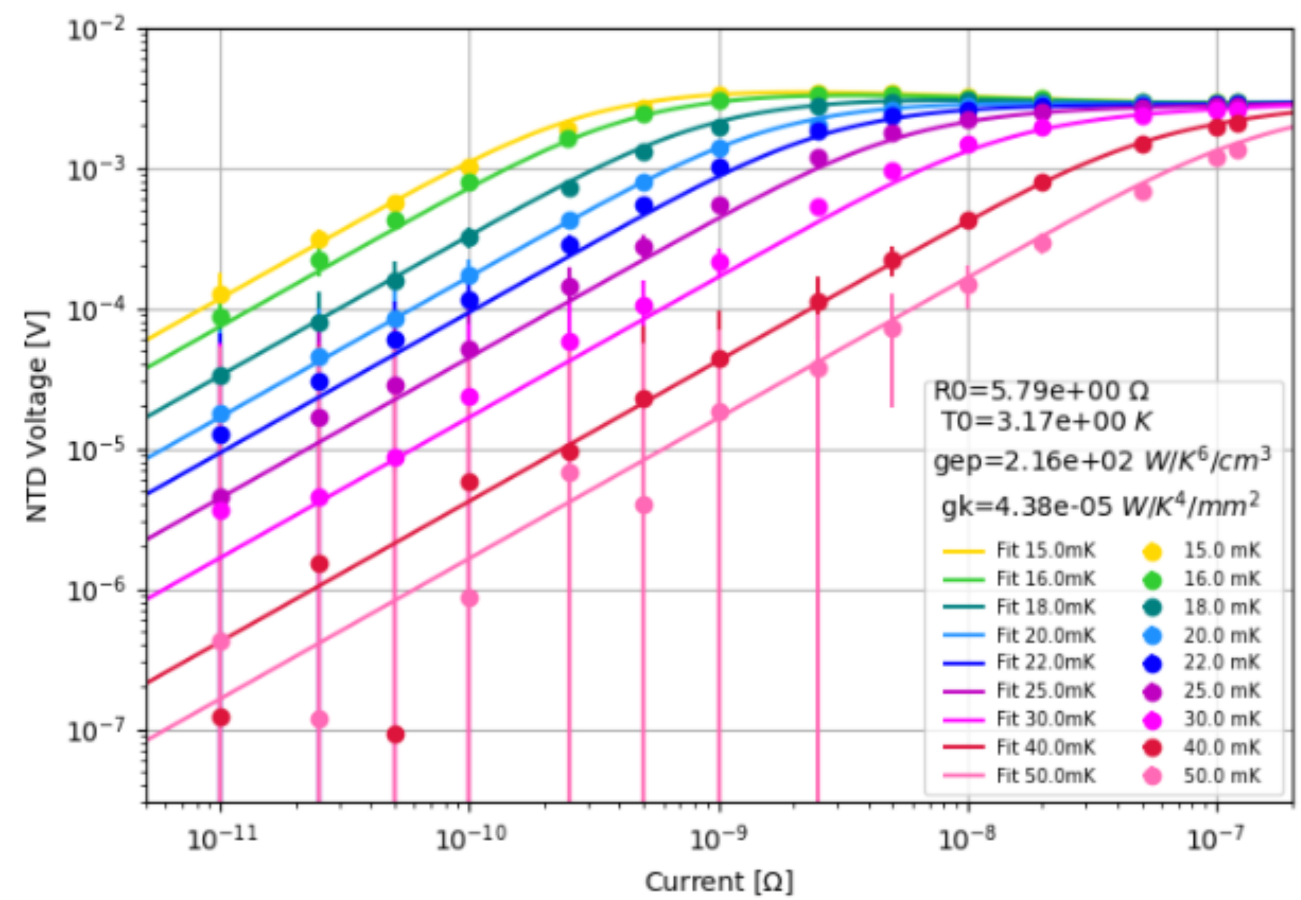

current [A]

Part II: Illustration with Ricochet detectors

1st order perturbation around equilibrium:

- Time domain solution

Linearization

Has to be solved thanks to linear algebra

$$\frac{d\mathbf{\Phi}}{dt} = -\mathbf{M}\mathbf{\Phi} + \mathbf{F}(t - t_0)$$

$$\frac{d\delta T_a}{dt} = -\frac{G^a_{ap}}{C_a}\delta T_a + \frac{G^p_{ap}}{C_a}\delta T_p$$

$$\frac{d\delta T_p}{dt} = \frac{G^a_{ap}}{C_p}\delta T_a - \frac{G^p_{ap} + G^p_{ep} + G^p_{pb}}{C_p}\delta T_p + \frac{G^e_{ep}}{C_p}\delta T_e$$

$$\frac{d\delta T_e}{dt} = \frac{G^p_{ep}}{C_e}\delta T_p - \frac{1}{C_e}\left(G^e_{ep} + \frac{\bar{V}^2}{R(\bar{T}_e)^2}\left.\frac{dR}{dT}\right|_{\bar{T}_e}\right)\delta T_e + 2\frac{1}{C_e}\frac{\bar{V}}{R(\bar{T}_e)}\delta V$$

$$\frac{d\delta V}{dt} = \frac{1}{C_{fil}}\frac{\bar{V}}{R(\bar{T}_e)^2}\left.\frac{dR}{dT}\right|_{\bar{T}_e}\delta T_e - \frac{1}{C_{fil}}\left(\frac{1}{R_L} + \frac{1}{R(\bar{T}_e)}\right)\delta V$$

G^i_j : Linearized conductivities

$$\boldsymbol{M} = \begin{pmatrix} \frac{G^a_{ap}}{C_a} & -\frac{G^p_{ap}}{C_a} & 0 & 0 \\ -\frac{G^a_{ap}}{C_p} & \frac{G^p_{ap}+G^p_{ep}+G^p_{pb}}{C_p} & -\frac{G^e_{ep}}{C_p} & 0 \\ 0 & -\frac{G^p_{ep}}{C_e} & \frac{1}{C_e}\left(G^e_{ep} + \frac{V^2}{R(T_e)^2}\left.\frac{dR}{dT}\right|_{T_e}\right) & -2\frac{V}{R(T_e)} \\ 0 & 0 & -\frac{1}{C_{fil}}\frac{V}{R(T_e)^2}\left.\frac{dR}{dT}\right|_{T_e} & \frac{1}{C_{fil}}\left(\frac{1}{R_L} + \frac{1}{R(T_e)}\right) \end{pmatrix}$$

Coupling matrix

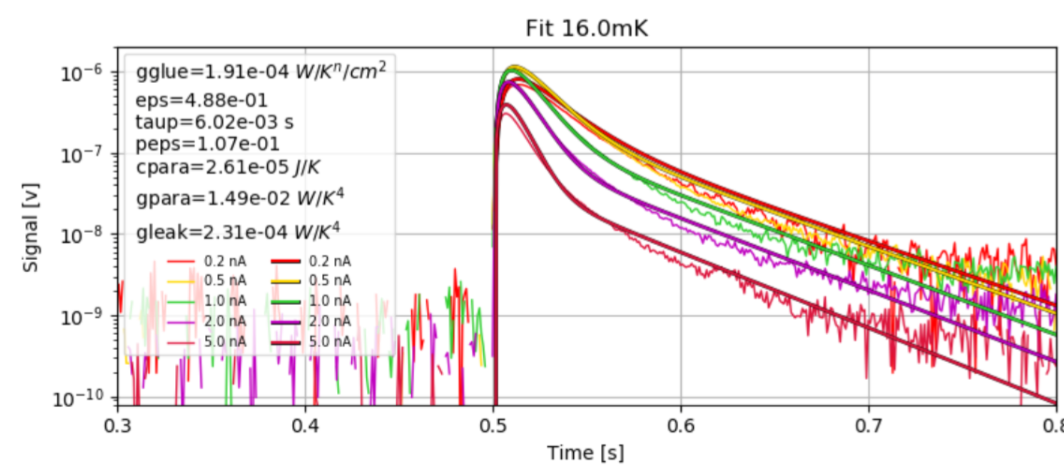

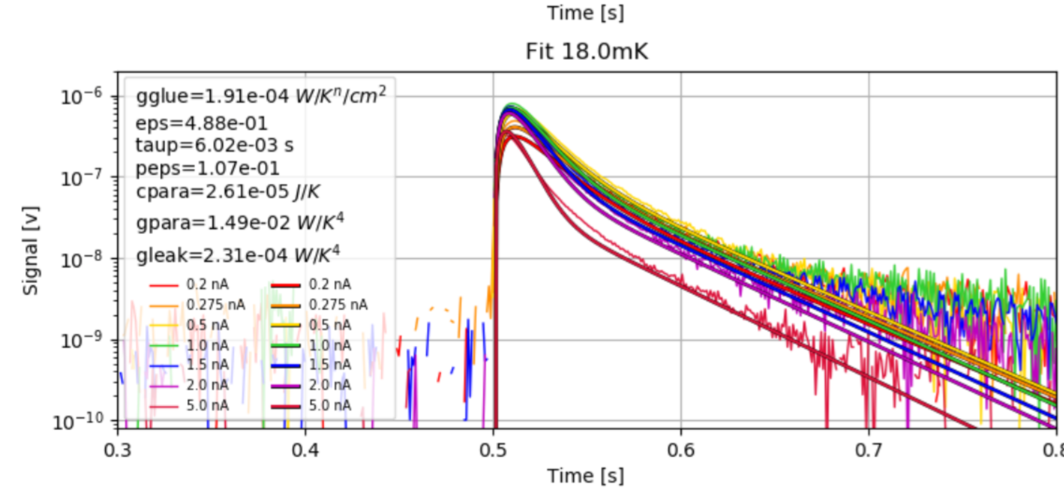

$$\boldsymbol{\phi} = \begin{pmatrix} \Delta T_a \\ \Delta T_p \\ \Delta T_e \\ \Delta V \end{pmatrix}$$

State vector

$$\boldsymbol{F}(t - t_0) = \begin{pmatrix} (1-\epsilon)E/C_a \\ 0 \\ \epsilon E/C_e \\ 0 \end{pmatrix}\delta(t - t0)$$

Initial perturbation

Part II: Illustration with Ricochet detectors

1st order perturbation around equilibrium:
- *Frequency domain (noise treatment)*

Fourier Transform of the differential equations

$$(i\omega + \mathbf{M})\tilde{\mathbf{\Phi}}(\omega) = \tilde{\mathbf{F}}(\omega) \longrightarrow \tilde{\mathbf{\Phi}}(\omega) = \mathbf{Z}^{-1}(\omega)\tilde{\mathbf{F}}(\omega)$$

$$\begin{pmatrix} \Delta\tilde{T}_a \\ \Delta\tilde{T}_p \\ \Delta\tilde{T}_e \\ \Delta\tilde{V} \end{pmatrix} = \begin{pmatrix} Z^{-1}_{aa} & Z^{-1}_{ap} & Z^{-1}_{ae} & Z^{-1}_{av} \\ Z^{-1}_{pa} & Z^{-1}_{pp} & Z^{-1}_{pe} & Z^{-1}_{pv} \\ Z^{-1}_{ea} & Z^{-1}_{ep} & Z^{-1}_{ee} & Z^{-1}_{ev} \\ Z^{-1}_{va} & Z^{-1}_{vp} & Z^{-1}_{ve} & Z^{-1}_{vv} \end{pmatrix} \begin{pmatrix} \Delta\tilde{P}_a \\ \Delta\tilde{P}_p \\ \Delta\tilde{P}_e \\ \Delta\tilde{I} \end{pmatrix} = \boldsymbol{Z}^{-1}(\omega)\tilde{\boldsymbol{F}}(\omega)$$

Total noise referenced to the NTD voltage:

$$S_{V,total} = \sum_i^{sources} \left| \sum_j^{a,p,e,v} Z^{-1}_{v,j}(\omega)\tilde{F}_j(\omega) \right|^2 \qquad [V^2/Hz]$$

Johnson Noise from NTD and load resistor

$$S_{V,R(T_e)} = \frac{4k_B T_e R(T_e)}{R(T_e)^2}\left|Z^{-1}_{vv}\right|^2 \quad S_{V,R_L} = \frac{4k_B T_{R_L} R_L}{R_L^2}\left|Z^{-1}_{vv}\right|^2$$

Thermal Fluctuation Noise (TFN)

$$S_{P,ij} = 2k_B(T_i^2 + T_j^2)G_{ij} \qquad [W^2/Hz]$$

To be referenced to V_{NTD}

Noise from the electronics

$$S_{V,e_{ampli.}} = e^2_{ampli.} \qquad S_{V,i_{ampli.}} = i^2_{ampli.}\left|Z^{-1}_{vv}\right|^2$$

Requires an accurate characterization of the electronics

Based on D. Misiak, PhD

Part II: Illustration with Ricochet detectors

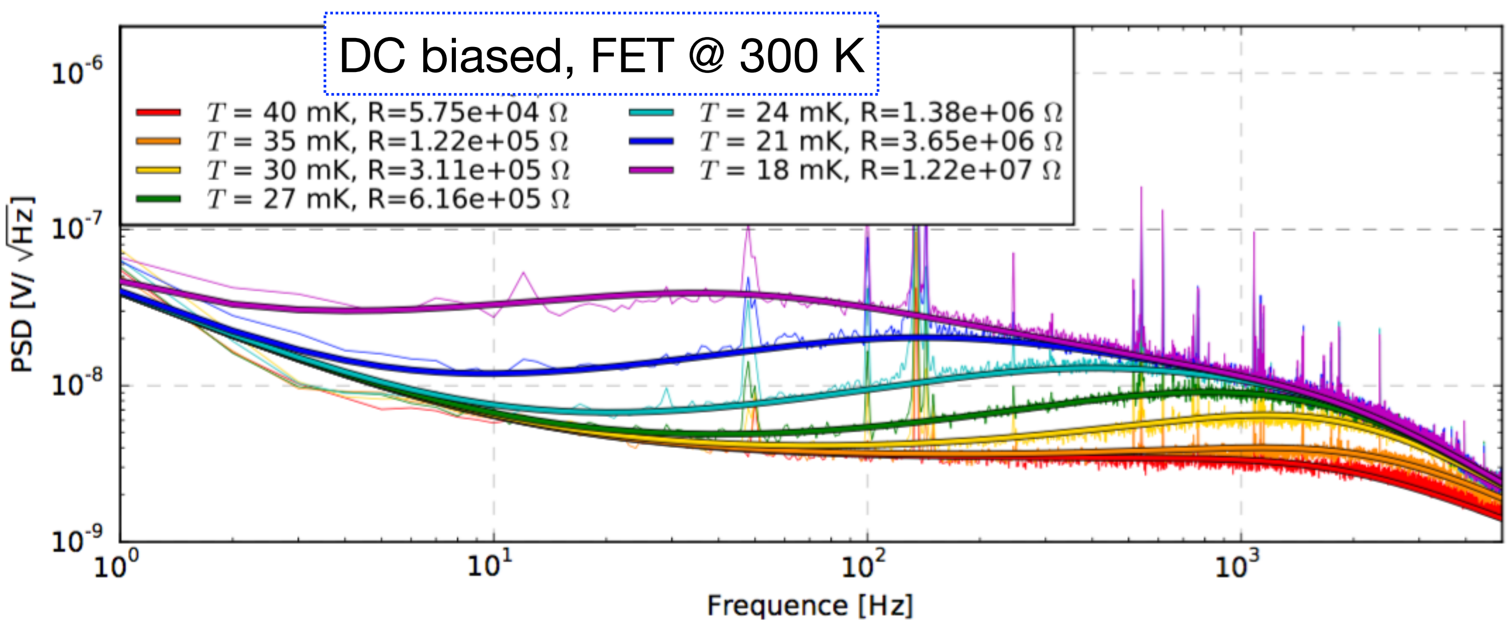

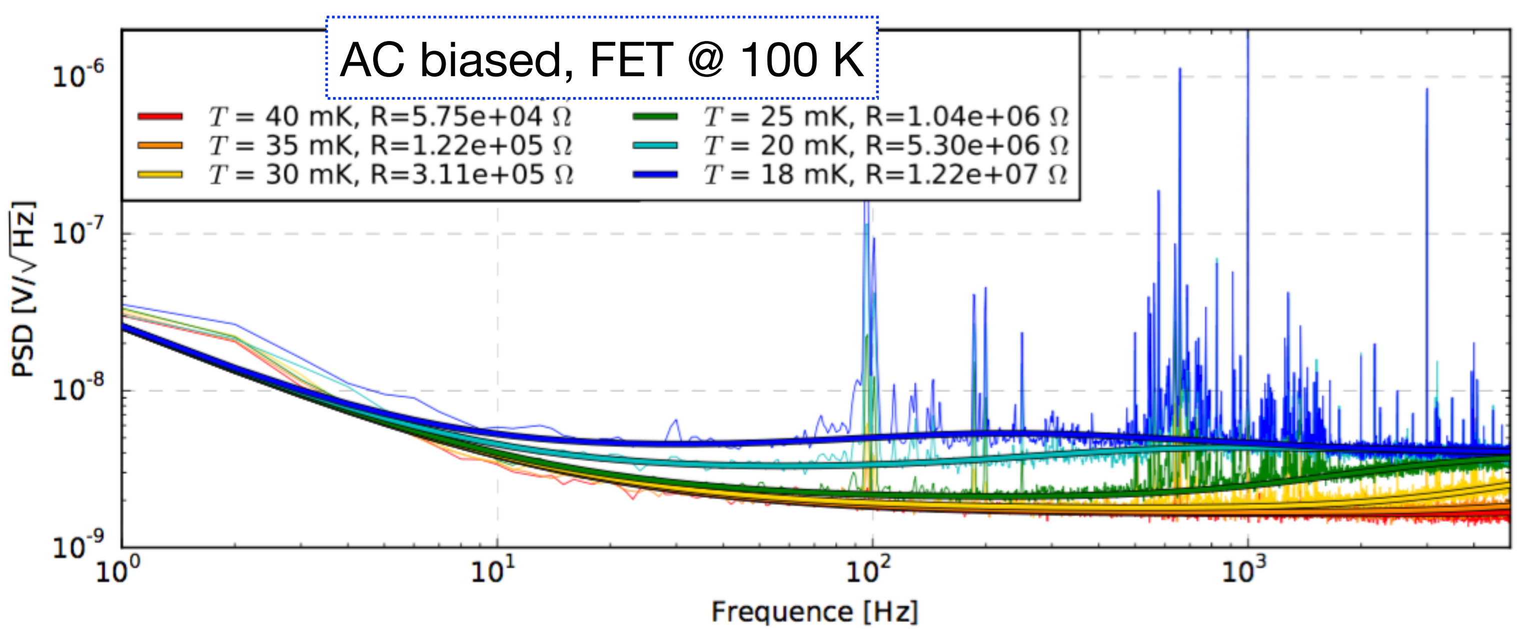

Thevenin-Norton transform:

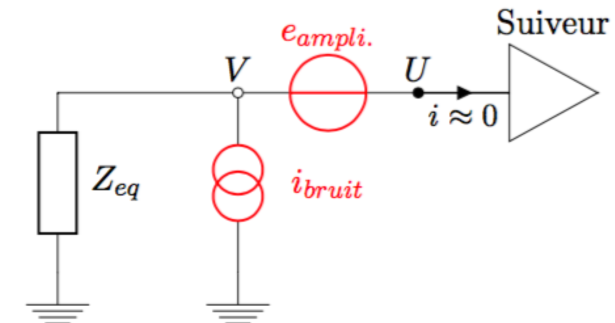

$$Z_{eq} = \left(\frac{1}{R_L} + \frac{1}{R(T_e)} + i\omega C_{fil}\right)^{-1}$$

$$i^2_{bruit} = i^2_{ampli} + \left(\frac{e_{J_{R_L}}}{R_L}\right)^2 + \left(\frac{e_{J_{NTD}}}{R(T_e)}\right)^2 \qquad [A^2/Hz]$$

$$i^2_{ampli.} = i^2_A + (i_B\sqrt{f})^2 + (i_C f)^2 \qquad [A^2/Hz]$$

$$e^2_{ampli.} = e^2_A + e^2_{BF} = e^2_A + \left(\frac{e_B}{\sqrt{f}}\right)^2 + \left(\frac{e_C}{f}\right)^2 \qquad [V^2/Hz]$$

- Work with Ip = 0 to cancel TFN and ETF contributions
- Scan in T to scan in Zeq to adjust free parameters thanks to **Markov Chain Monte Carlo approach**

Clear gain in intrinsic electronic noise by working with FET @ 100 K:

~3 nV/sqrt{Hz} @ 10 - 100 Hz with R_{NTD} = 5 MOhm

Based on D. Misiak, PhD

Part II: Illustration with Ricochet detectors

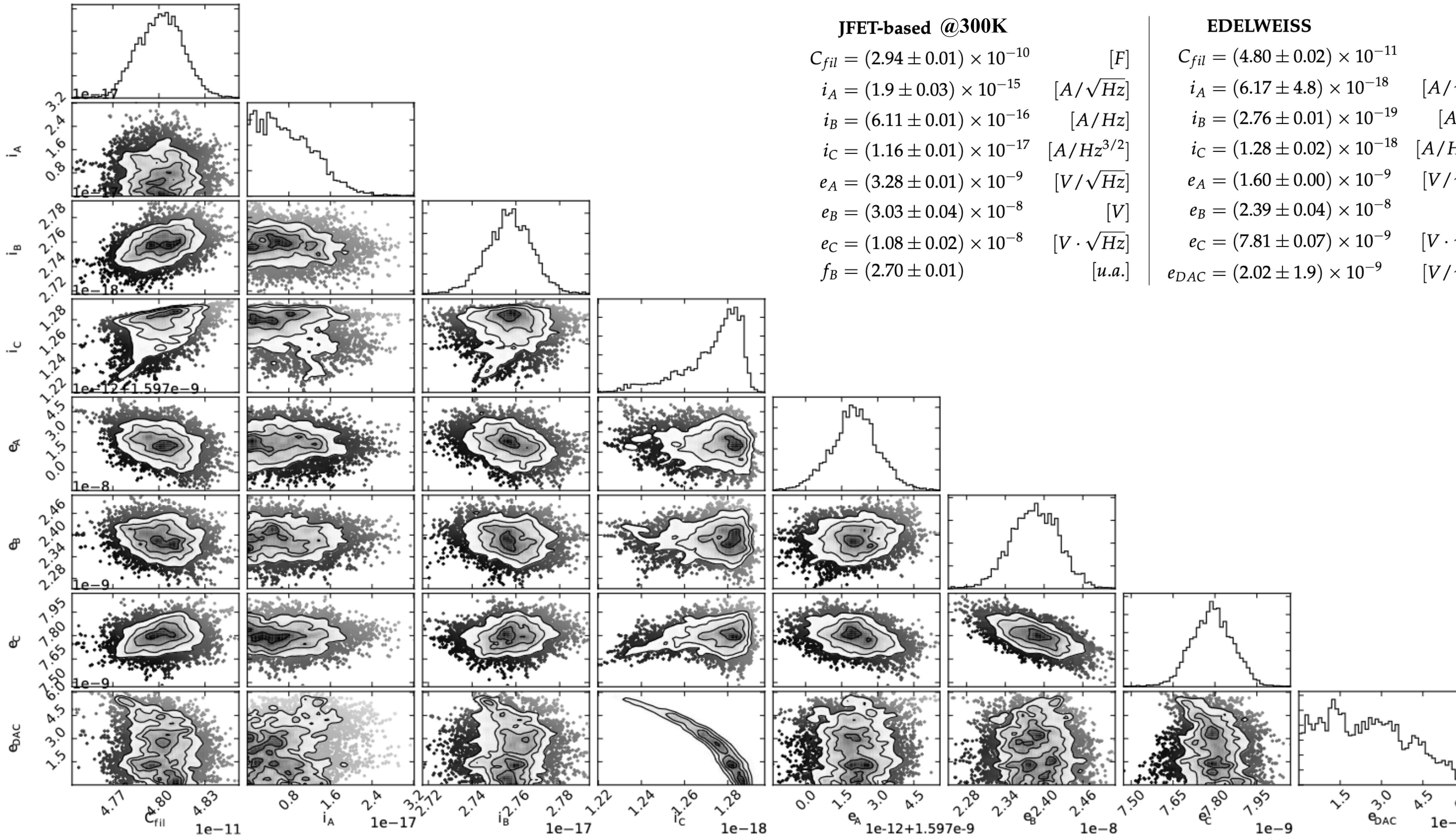

JFET-based @300K		**EDELWEISS**	
$C_{fil} = (2.94 \pm 0.01) \times 10^{-10}$	$[F]$	$C_{fil} = (4.80 \pm 0.02) \times 10^{-11}$	$[F]$
$i_A = (1.9 \pm 0.03) \times 10^{-15}$	$[A/\sqrt{Hz}]$	$i_A = (6.17 \pm 4.8) \times 10^{-18}$	$[A/\sqrt{Hz}]$
$i_B = (6.11 \pm 0.01) \times 10^{-16}$	$[A/Hz]$	$i_B = (2.76 \pm 0.01) \times 10^{-19}$	$[A/Hz]$
$i_C = (1.16 \pm 0.01) \times 10^{-17}$	$[A/Hz^{3/2}]$	$i_C = (1.28 \pm 0.02) \times 10^{-18}$	$[A/Hz^{3/2}]$
$e_A = (3.28 \pm 0.01) \times 10^{-9}$	$[V/\sqrt{Hz}]$	$e_A = (1.60 \pm 0.00) \times 10^{-9}$	$[V/\sqrt{Hz}]$
$e_B = (3.03 \pm 0.04) \times 10^{-8}$	$[V]$	$e_B = (2.39 \pm 0.04) \times 10^{-8}$	$[V]$
$e_C = (1.08 \pm 0.02) \times 10^{-8}$	$[V \cdot \sqrt{Hz}]$	$e_C = (7.81 \pm 0.07) \times 10^{-9}$	$[V \cdot \sqrt{Hz}]$
$f_B = (2.70 \pm 0.01)$	$[u.a.]$	$e_{DAC} = (2.02 \pm 1.9) \times 10^{-9}$	$[V/\sqrt{Hz}]$

Part II: Illustration with Ricochet detectors

1st order perturbation around equilibrium:

- *Frequency domain (noise treatment)*

Fourier Transform of the differential equations

$$(i\omega + \mathbf{M})\tilde{\mathbf{\Phi}}(\omega) = \tilde{\mathbf{F}}(\omega) \longrightarrow \tilde{\mathbf{\Phi}}(\omega) = \mathbf{Z}^{-1}(\omega)\tilde{\mathbf{F}}(\omega)$$

$$\begin{pmatrix} \Delta\tilde{T}_a \\ \Delta\tilde{T}_p \\ \Delta\tilde{T}_e \\ \Delta\tilde{V} \end{pmatrix} = \begin{pmatrix} Z^{-1}_{aa} & Z^{-1}_{ap} & Z^{-1}_{ae} & Z^{-1}_{av} \\ Z^{-1}_{pa} & Z^{-1}_{pp} & Z^{-1}_{pe} & Z^{-1}_{pv} \\ Z^{-1}_{ea} & Z^{-1}_{ep} & Z^{-1}_{ee} & Z^{-1}_{ev} \\ Z^{-1}_{va} & Z^{-1}_{vp} & Z^{-1}_{ve} & Z^{-1}_{vv} \end{pmatrix} \begin{pmatrix} \Delta\tilde{P}_a \\ \Delta\tilde{P}_p \\ \Delta\tilde{P}_e \\ \Delta\tilde{I} \end{pmatrix} = \boldsymbol{Z}^{-1}(\omega)\tilde{\boldsymbol{F}}(\omega)$$

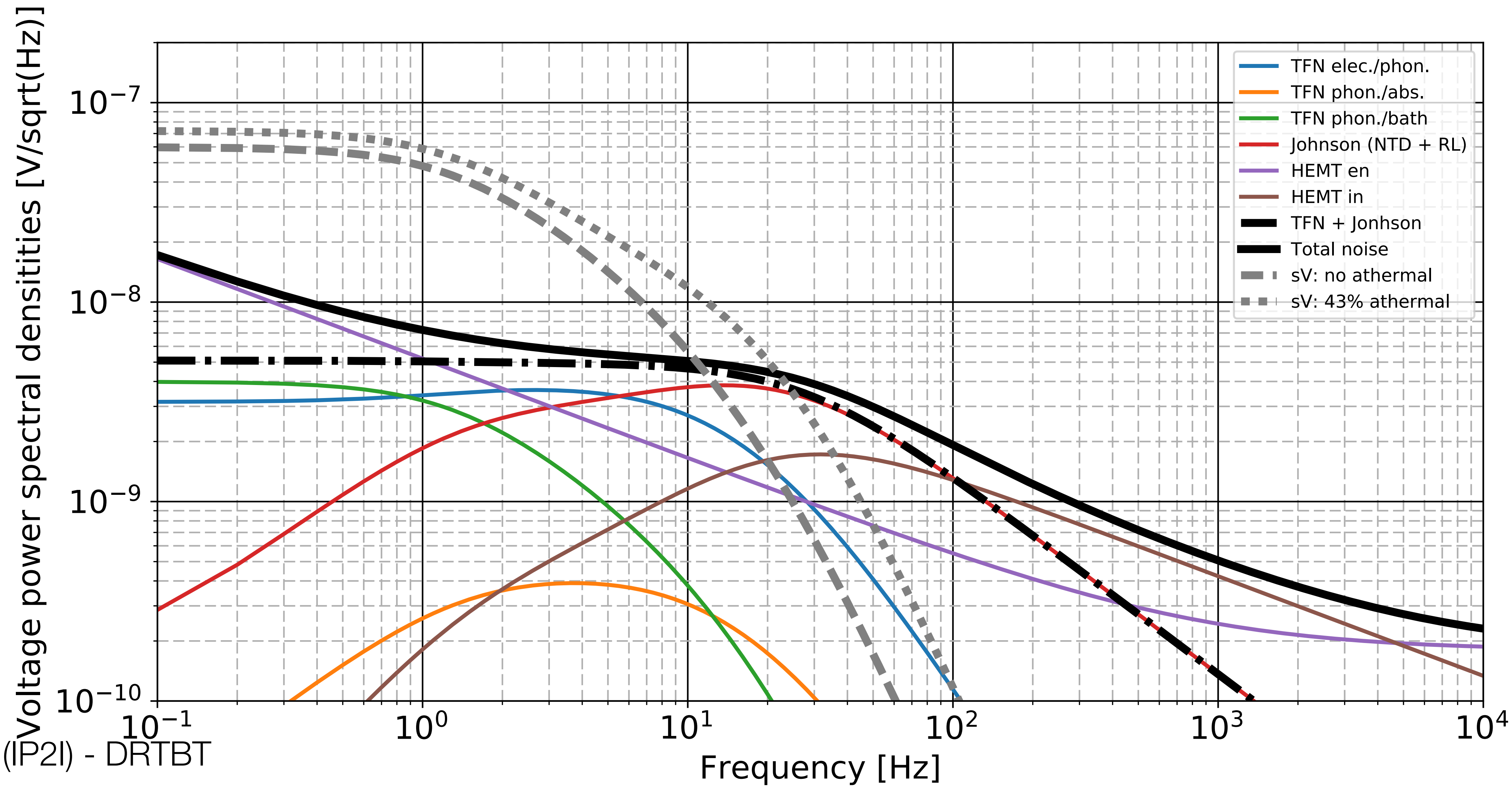

Part II: Illustration with Ricochet detectors

A concrete example with a simple detector: RED20

1st order perturbation around equilibrium:

- Frequency domain (noise treatment)

$$(i\omega + \mathbf{M})\tilde{\mathbf{\Phi}}(\omega) = \tilde{\mathbf{F}}(\omega) \longrightarrow \tilde{\mathbf{\Phi}}(\omega) = \mathbf{Z}^{-1}(\omega)\tilde{\mathbf{F}}(\omega)$$

Fourier Transform of the differential equations

$$\begin{pmatrix} \Delta\tilde{T}_a \\ \Delta\tilde{T}_p \\ \Delta\tilde{T}_e \\ \Delta\tilde{V} \end{pmatrix} = \begin{pmatrix} Z^{-1}_{aa} & Z^{-1}_{ap} & Z^{-1}_{ae} & Z^{-1}_{av} \\ Z^{-1}_{pa} & Z^{-1}_{pp} & Z^{-1}_{pe} & Z^{-1}_{pv} \\ Z^{-1}_{ea} & Z^{-1}_{ep} & Z^{-1}_{ee} & Z^{-1}_{ev} \\ Z^{-1}_{va} & Z^{-1}_{vp} & Z^{-1}_{ve} & Z^{-1}_{vv} \end{pmatrix} \begin{pmatrix} \Delta\tilde{P}_a \\ \Delta\tilde{P}_p \\ \Delta\tilde{P}_e \\ \Delta\tilde{I} \end{pmatrix} = \boldsymbol{Z}^{-1}(\omega)\tilde{\boldsymbol{F}}(\omega)$$

Detector sensitivity

$$\hat{s}_V(\omega) = \left[(1-\epsilon)Z^{-1}_{va} + \epsilon Z^{-1}_{ve}\right]\hat{p}(\omega)$$

Noise Equivalent Power (NEP)

$$\mathrm{NEP}^2(\omega) = \frac{S_{V,total}(\omega)}{|s_V|^2} \qquad \mathrm{W}^2/\mathrm{Hz}$$

Theoretical energy resolution (RMS)

$$\sigma_E^2 = \left(\int_0^\infty \frac{d\omega}{2\pi}\frac{4}{|\mathrm{NEP}|^2(\omega)}\right)^{-1}$$

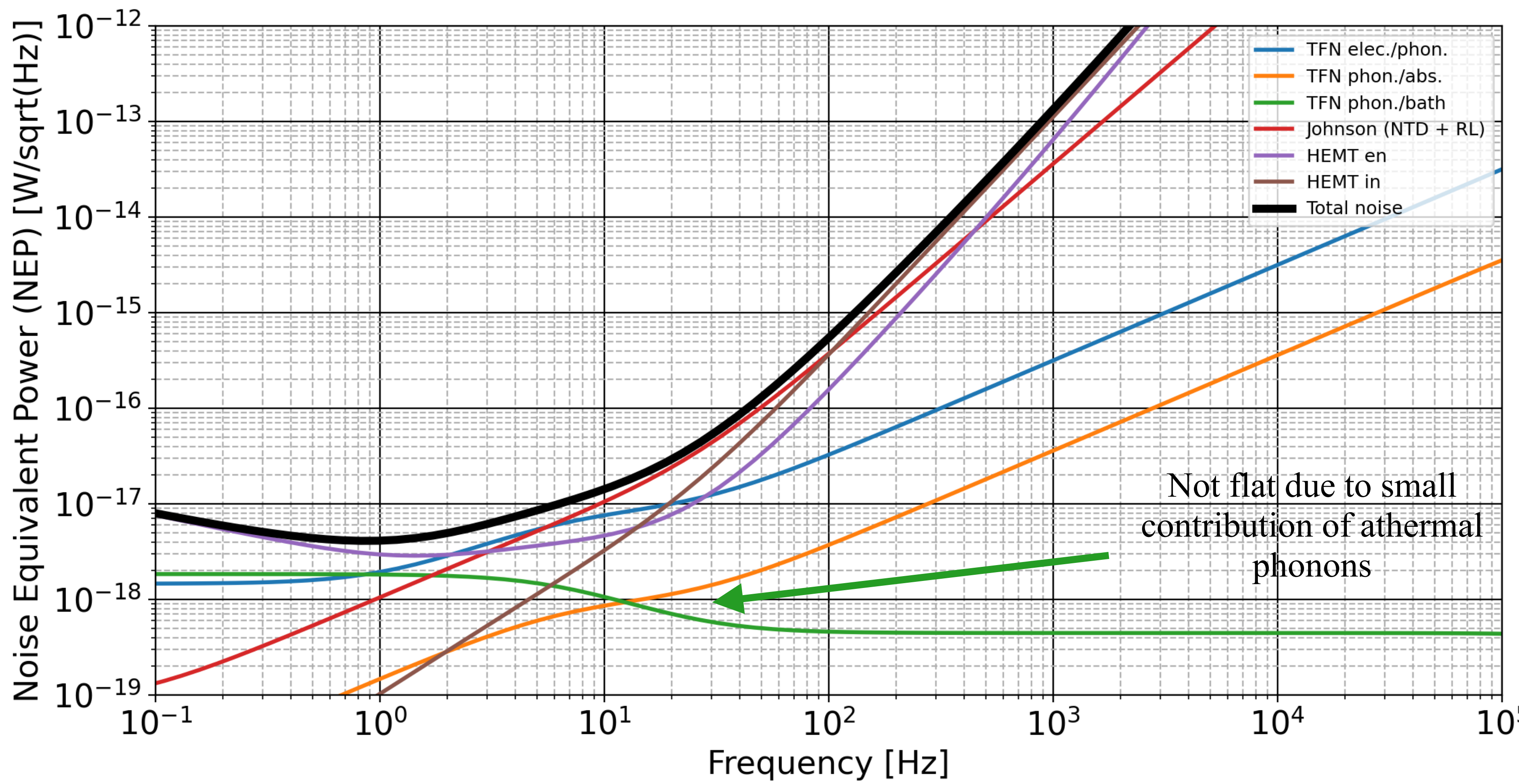

Part II: Illustration with Ricochet detectors

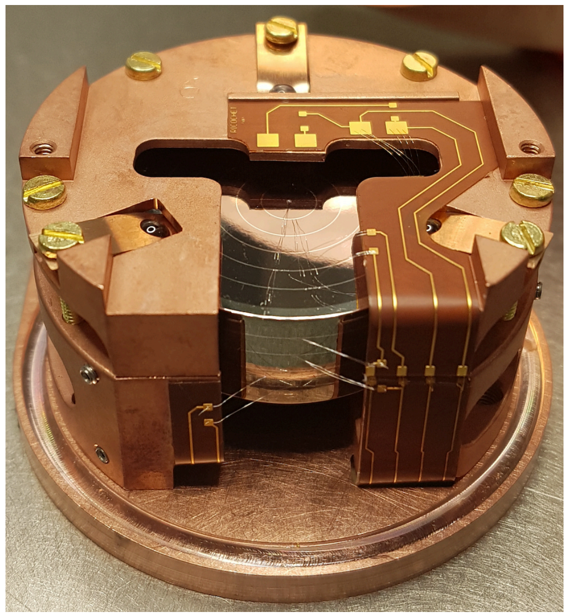

- Expected energy resolution around 10 eV
- Leading to a (5sigma) threshold of 50 eV

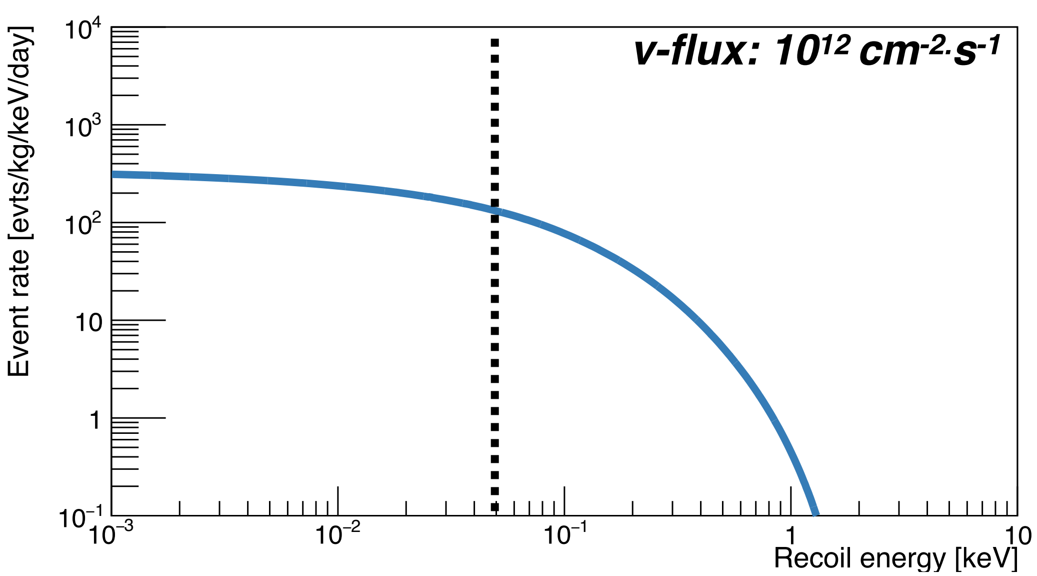

Component	Value	Notes
Bath		
Temperature	13 mK	
Absorber	Ge	
Volume	$\pi \times 2^2/4 \times 2 = 6.3$ cm^3	33.4 g
Heat capacity	$C_a = 5.97 \times 10^{-11}$ J/K	$C_a = 2.7 \times 10^{-6}\bar{T}_a^3$ J/K/cm^3
NTD	Ge	
Surface (S_{NTD})	$2 \times 2 = 4$ mm^2	
Thickness	0.45 mm	
Volume (V_{NTD})	1.8 mm^3	
Surface electrodes (S_{Au})	$2 \times (0.15 \times 2) = 0.6$ mm^2	
R_0 / T_0	0.96 Ω / 4.52 K	$\bar{R}(\bar{T}_e) = R_0 e^{\sqrt{T_0/\bar{T}_e}}$
Heat capacity (phonon)	$C_p = 1.71 \times 10^{-14}$ J/K	$C_p = 2.7 \times 10^{-6}\bar{T}_p^3$ J/K/cm^3
Heat capacity (electron)	$C_e = 3.17 \times 10^{-11}$ J/K	$C_e = 1.1 \times 10^{-6}\bar{T}_e$ J/K/cm^3
Conductivities		
Electron-Phonon (NTD)	$G_{ep}^e \approx G_{ep}^p = 1.12$ nW/K	$g_{ep} = 100$ W/K^6/cm^3
Phonon (NTD-Abs.)	$G_{pa}^a = G_{pa}^p = 55.9$ nW/K	$g_{glue} = 1.4 \times 10^{-4}$ W/K$^{3.5}$/mm^2
Phonon (Abs-Bath)	$G_{pb} = 0.42$ nW/K	$g_k = 5 \times 10^{-5}$ W/K^4/mm^2
Equilibrium state $\phi(0)$		
NTD-electron	$\bar{T}_e = 15.9$ mK	
NTD-phonon	$\bar{T}_p = 15.2$ mK	
Absorber	$\bar{T}_a = 15.2$ mK	
Voltage	$\bar{V} = 3.82$ mV	$\bar{V} = V_b\bar{R}/(R_L + \bar{R})$
Electronic considerations		
Voltage bias	$V_b = 0.2$ V	$I_p = V_b/(R_L + \bar{R}) \approx 0.2$ nA
Load resistor	$R_L = 1$ GΩ	$T_{R_L} = 13$ mK
NTD Resistance	$\bar{R} = 19.48$ MΩ	$\bar{R} = R(\bar{T}_e)$
IF1320-JFET ($C_{tot} = 50$ pF)	$e_n^2 = e_a^2 + e_b^2/f$	$\{e_a, e_b\} = \{0.5, 7.3\}$ nV/$\sqrt{\text{Hz}}$
	$i_n^2 = i_a^2 + i_b^2 \times f$	$\{i_a, i_b\} = \{18, 50\}$ aA/$\sqrt{\text{Hz}}$
200pF-HEMT ($C_{tot} = 250$ pF)	$e_n^2 = e_a^2 + e_b^2/f$	$\{e_a, e_b\} = \{0.18, 5.2\}$ nV/$\sqrt{\text{Hz}}$
	$i_n^2 = i_a^2 + i_b^2 \times f$	$\{i_a, i_b\} = \{8.2 \times 10^{-4}, 21\}$ aA/$\sqrt{\text{Hz}}$
Time constants of the system		driven by :
1st eigenvalue	$\tau_1 = 0.3\ \mu$s	$\tau_{ap} = C_p/G_{ap} = 0.3\ \mu$s
2nd eigenvalue	$\tau_2 = 118.7$ ms	$\tau_{ab} = C_a/(G_{pb} \parallel G_{ap}) = 143.2$ ms
3rd eigenvalue	$\tau_3 = 16.4$ ms	$\tau_{ep} = C_e/G_{ep} = 28.2$ ms
4th eigenvalue (FET)	$\tau_4 = 979\ \mu$s	$\tau_{elec.} = \bar{R}C_c = 974\ \mu$s
4th eigenvalue (HEMT)	$\tau_4 = 5.7$ ms	$\tau_{elec.} = \bar{R}C_c = 5$ ms
Energy resolutions (RMS)	$\epsilon = 0 \mid (\epsilon = 0.43, \tau_p = 6$ ms$)$	$\epsilon \neq 0$ to match observations (Sec. 5.3)
Sensitivity [μV/keV]	$s_V = 1.8 \mid s_V = 5$	Pulse height in time domain (with FET)
FET (DC)	$\sigma_E =$ **10.7 eV** $\mid \sigma_E =$ **7.6 eV**	
HEMT (DC)	$\sigma_E =$ **9.0 eV** $\mid \sigma_E =$ **6.3 eV**	
FET (AC)	$\sigma_E = 13.2$ eV $\mid \sigma_E = 9.9$ eV	400 Hz modulation
No elec. noise	$\sigma_E = 6.5$ eV $\mid \sigma_E = 4.8$ eV	Only TFN + Johnson noise
Theoretical limit	$\sigma_E = 1.7$ eV	$\sigma_E = \sqrt{k_B\bar{T}_a^2 C_a}$

Part II: Illustration with Ricochet detectors

Salagnac & al: arXiv:2111.12438

Threshold defined for all experiments as 5σ

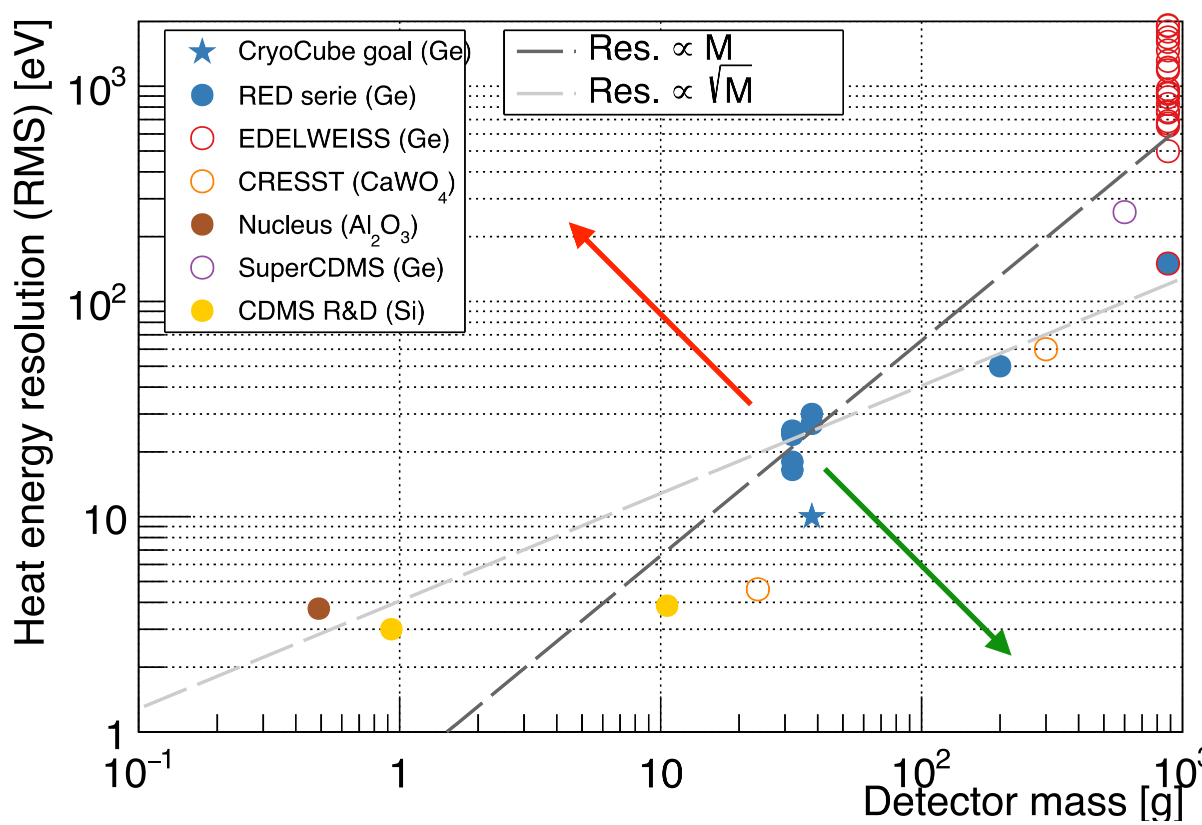

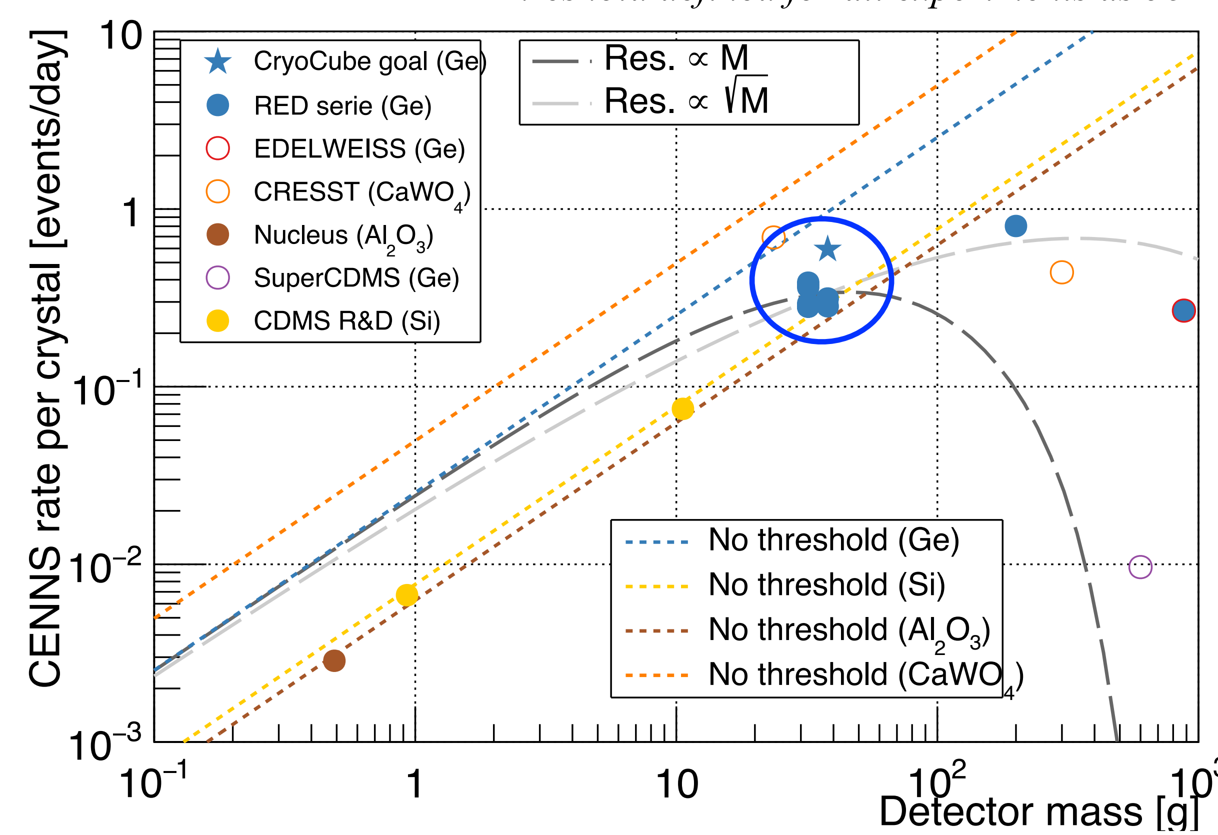

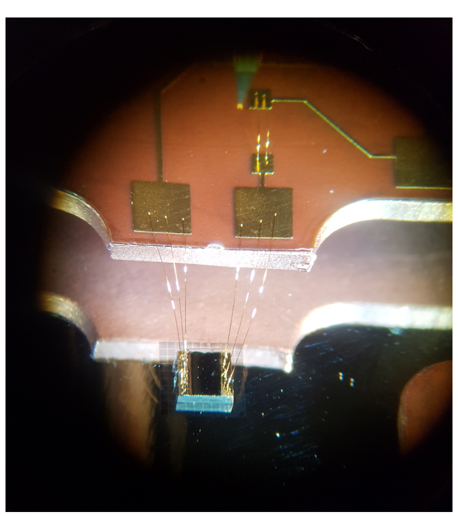

- Achieved 17 - 40 eV (RMS) heat resolution on 10 Ge detectors (38 g) with JFET electronics with **no cryogenic suspension**
- With respect to the community our detectors achieve among the **best resolution-to-mass ratio** and exhibit the **largest CENNS signal strength per crystal** from above ground operation of about 0.3 evt/day (goal 0.6 evt/day) 8.8m away from the ILL reactor.
- Our detector performance are still impacted from electrodes and environmental noise (vibrations, E&M pick ups) — ***See Jules C. for more details on data processing***

PART II: ILLUSTRATION WITH RICOCHET DETECTORS

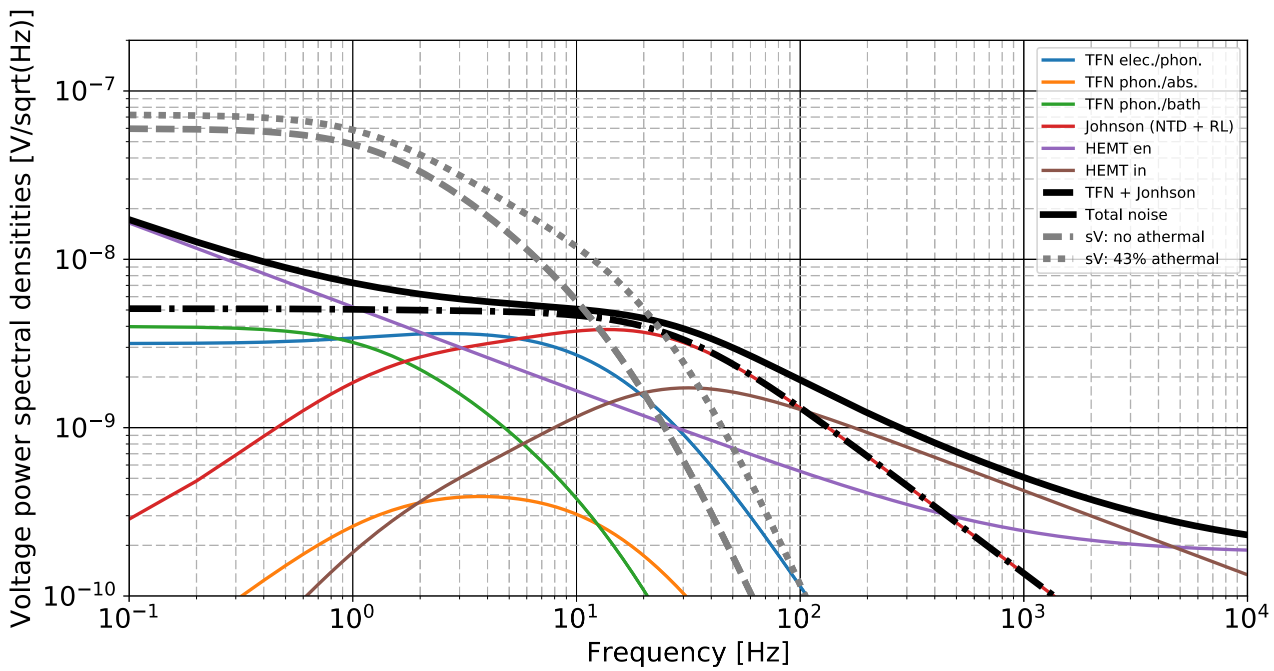

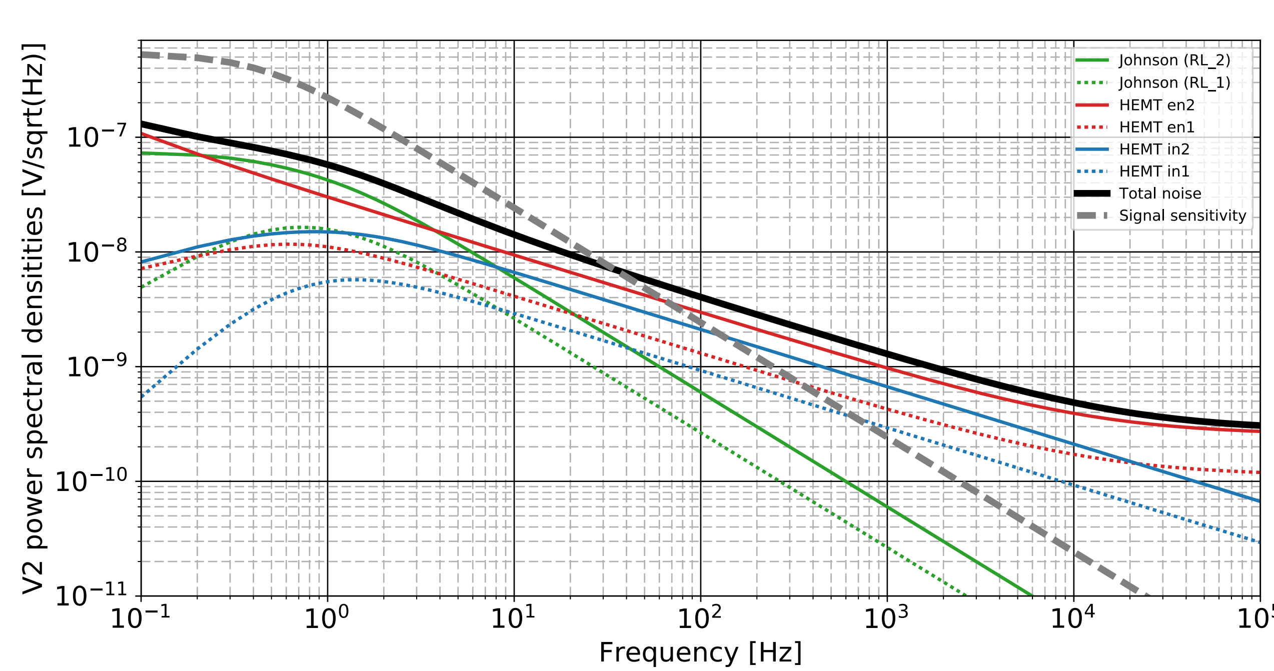

$$\sigma^2_{\hat{t}_0} = \left[\hat{a}^2 \int_{-\infty}^{+\infty} df \, (2\pi f)^2 \frac{|\tilde{A}(f)|^2}{J(f)}\right]^{-1}$$

- Timing resolution is very important for Ricochet because of active muon veto coincidence
- From noise and signal power spectral densities (PSD) we can derive the timing resolutions:
  - *High sampling frequency helps the ionization timing resolution*
  - *No gain in timing resolution beyond few 100 Hz for heat*

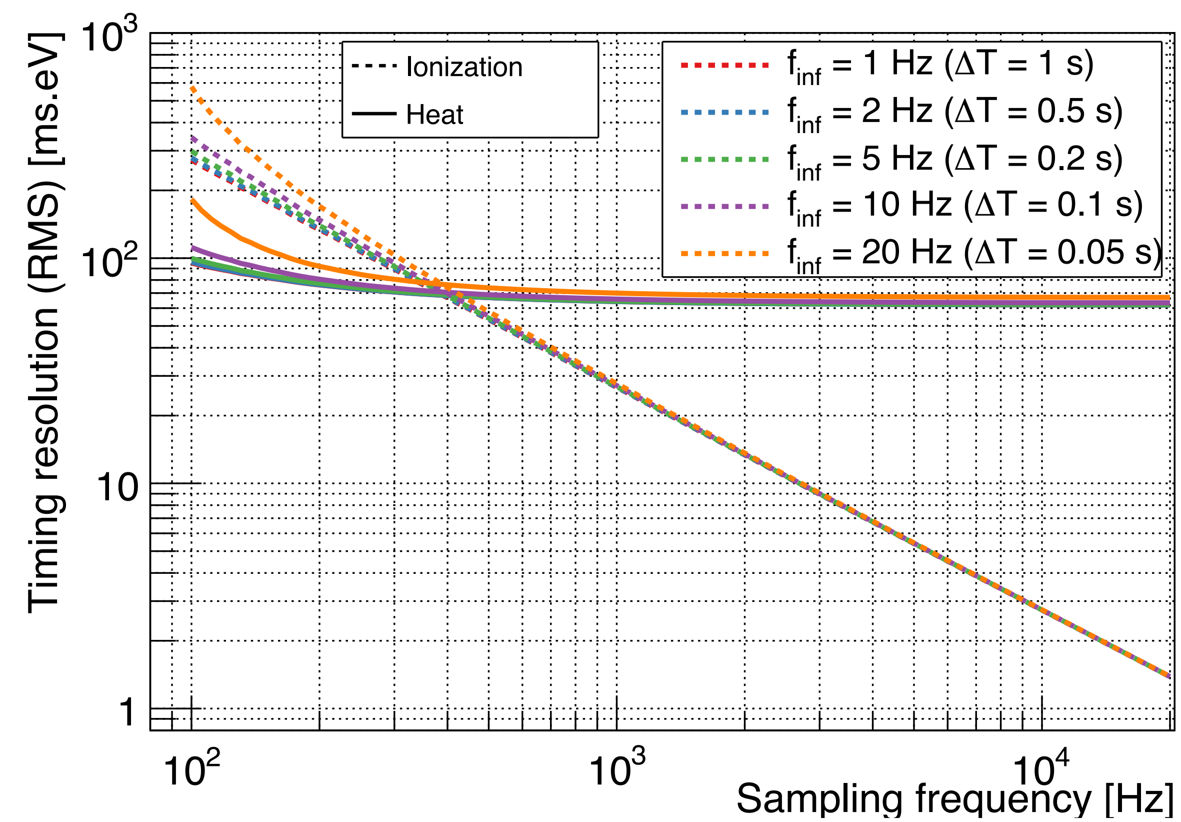

Part III: Other recent examples (active ETF)

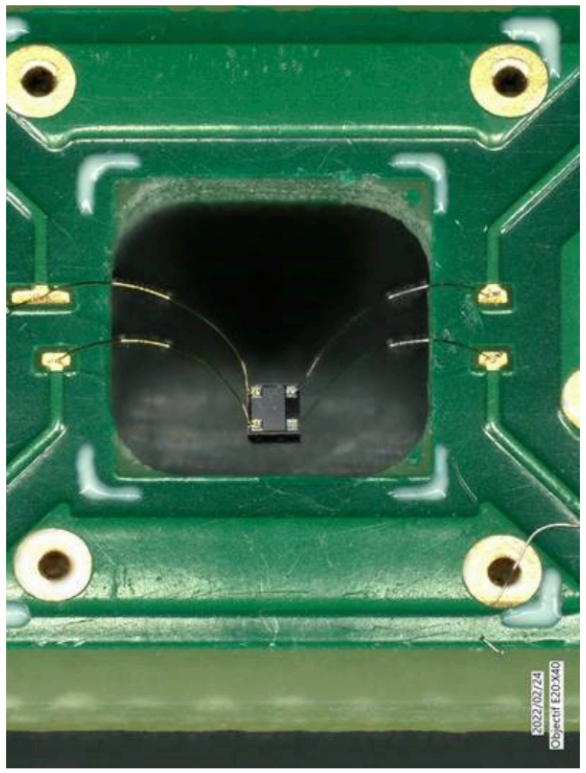

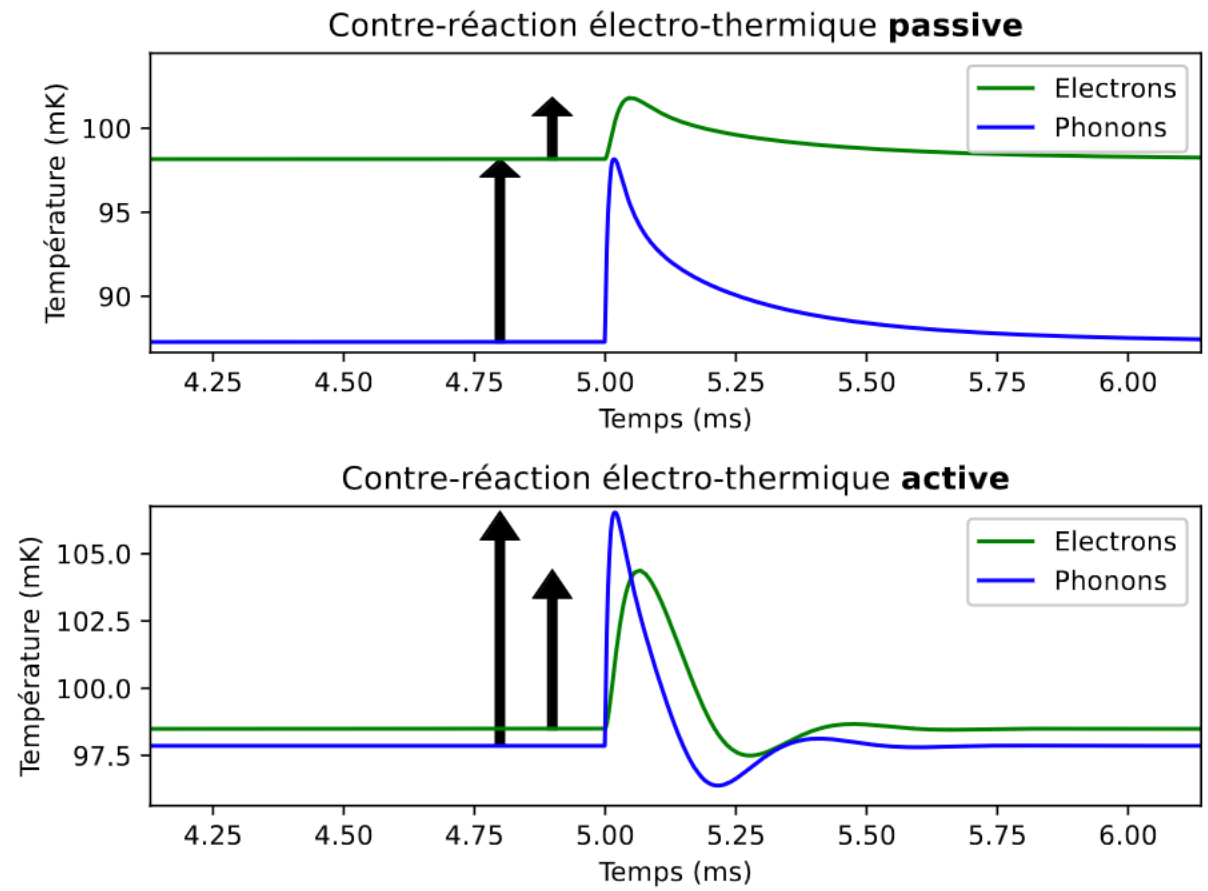

- Use of two NbSi high impedance TES to: measure the heat from particle interaction (thermometer) and to regulate the temperature actively (heater)
- The « thermometer » is then weakly current biased to minimise Te-Tp decoupling
- Use of the heater to actively stabilise the thermometer (active negative ETF)
- For more details, see PhD theses from: G. Jego and B. Criton (CEA Saclay)

Based on B. Criton, PhD

PART III: OTHER RECENT EXAMPLES (ACTIVE ETF)

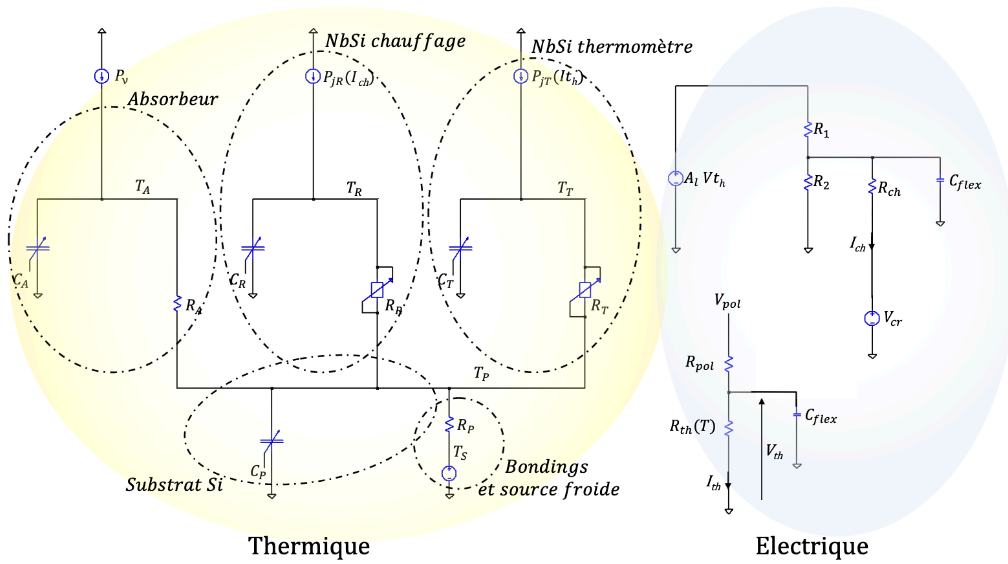

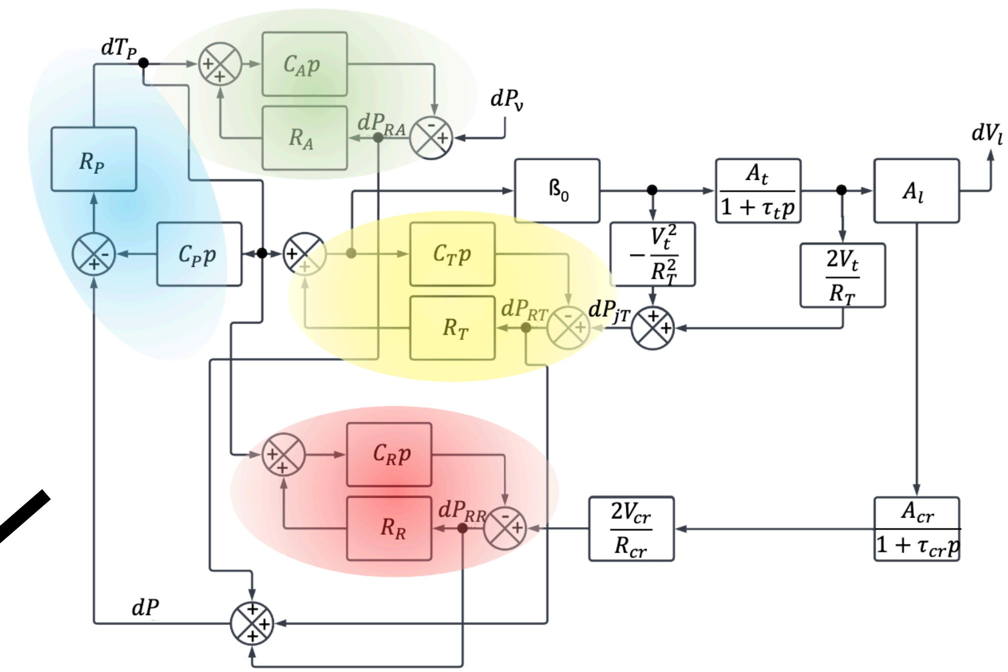

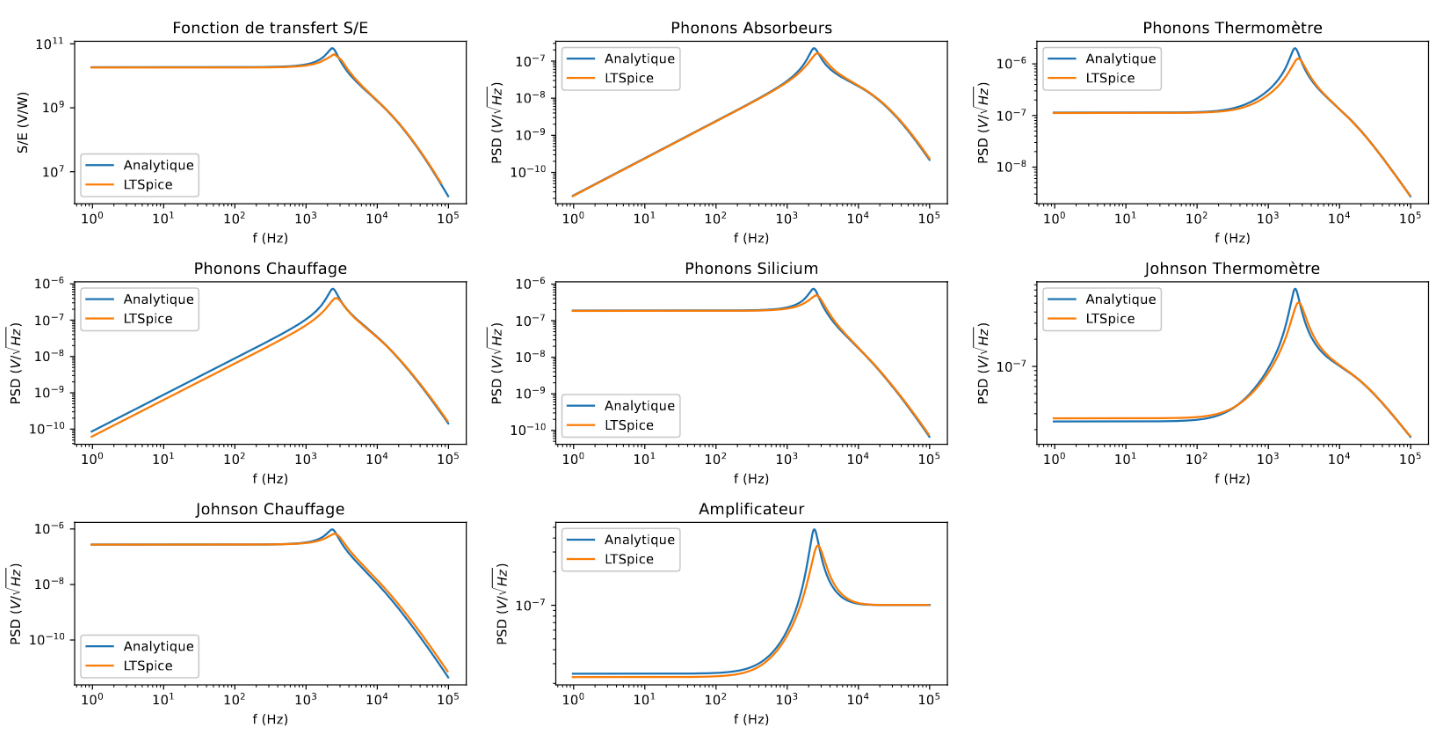

- Use of equivalence between thermal and electrical equations to use LTSpice
- Very good agreement between LTSPice and analytical model
- **Allows for detector parameter optimisation**

PART III: OTHER RECENT EXAMPLES (ACTIVE ETF)

Paramètre	Valeur
Température source froide	70 mK
Température des phonons	91.61 mK
Température des électrons thermomètre	92.21 mK
Température des électrons chauffage	109.15 mK
Résistance thermique source froide	10 GK/W
Constante de découplage	600
Volume NbSi thermomètre	3×10^{-9}cm^3
Volume NbSi chauffage	2×10^{-10}cm^3
Volume absorbeur	3×10^{-6}cm^3
Volume Silicium	1.25×10^{-6}cm^3
V_{pol}	10 mV
V_{cr}	-2.8 mV
R_{pol}	10 MΩ
R_{ch}	3 MΩ
dR/dT	150.1 GΩ/K
R_{th}	423.3 kΩ

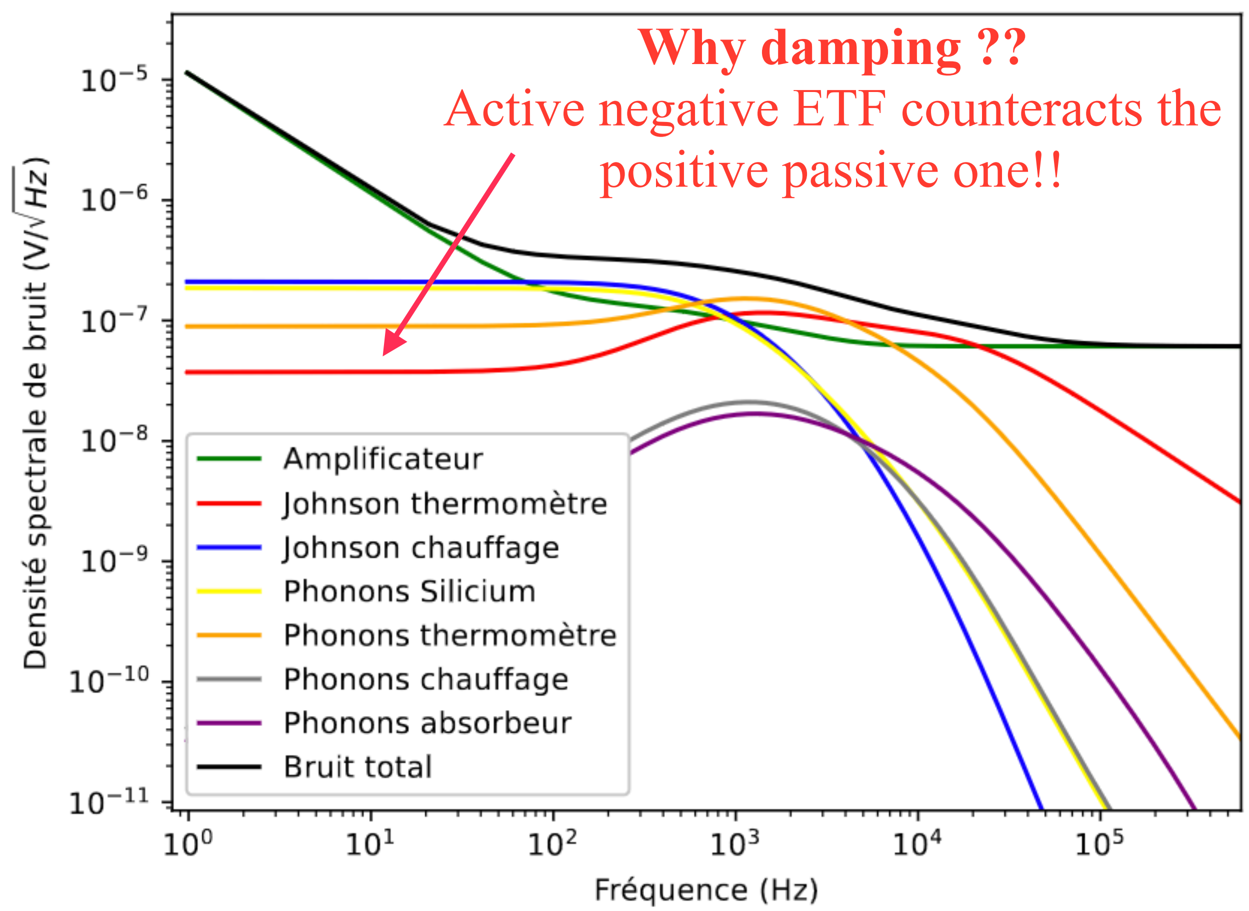

- Role of the active ETF very well demonstrated
- Expected energy resolution of 2.1 eV (FWHM)
- First results with a measured ~800 eV (FWHM) resolution with significant improvements planned ahead

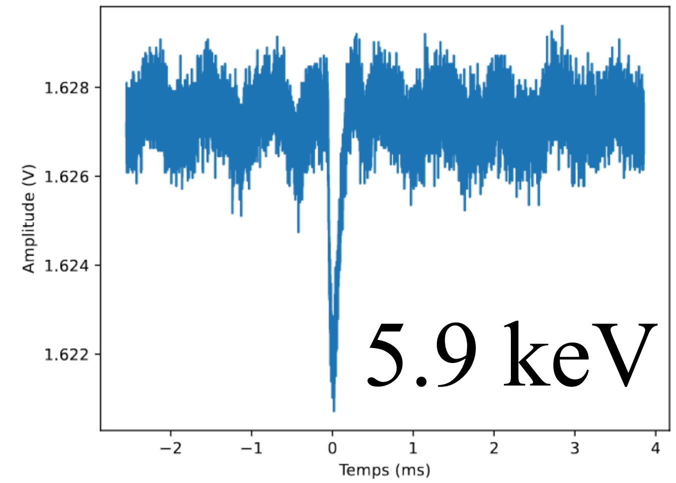

Figure 3.2.28 – Pulse d'un photon de Fer 55.

Part III: Other recent examples (DC power)

J. Billard, M. Pyle, S. Rajendran, H. Ramani, arXiv: arXiv:2208.05485

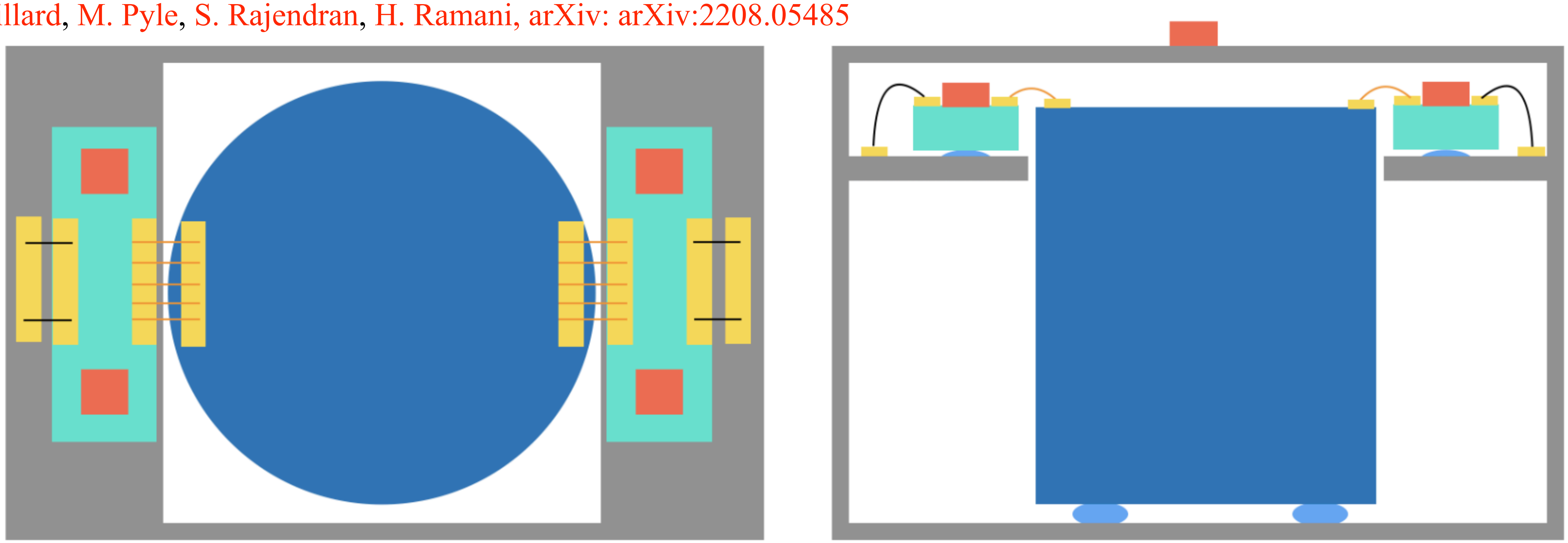

- Try to measure a DC power impinging on the crystal target
- Use of 2 sensing slabs with 2 NTDs each to
  - Measure precisely electrothermal responses and thermal conductivities
  - Reduce correlated noise
- Must allow for DM heating « ON » and « OFF » mode by simply breaking the wire bonds
- **Very very very difficult** measurement but this was a fun model to derive with potentially significant science reach

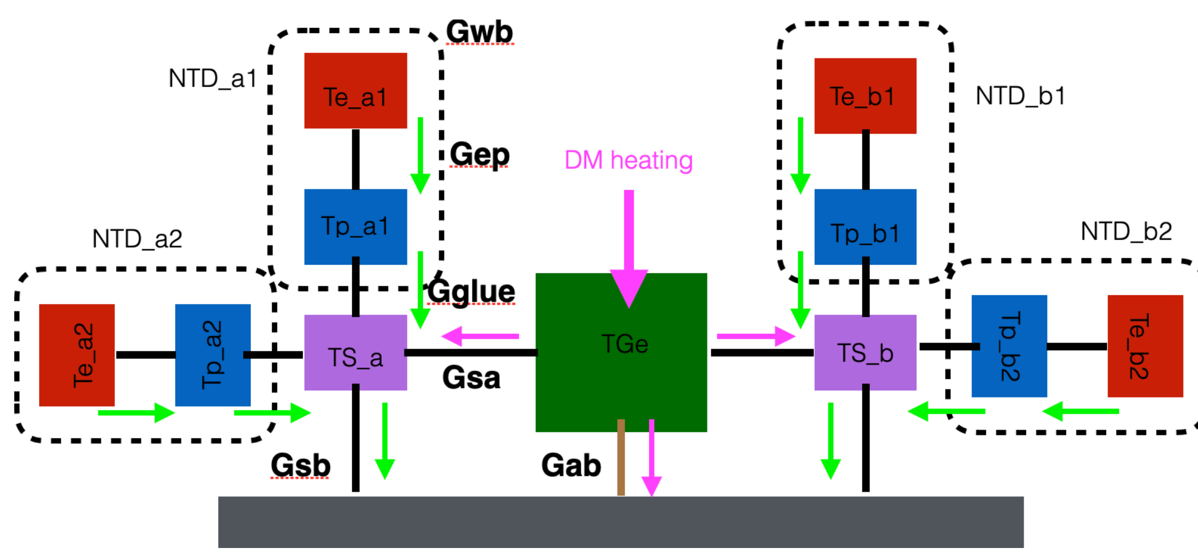

Part III: Other recent examples (DC power)

J. Billard, M. Pyle, S. Rajendran, H. Ramani, arXiv: arXiv:2208.05485

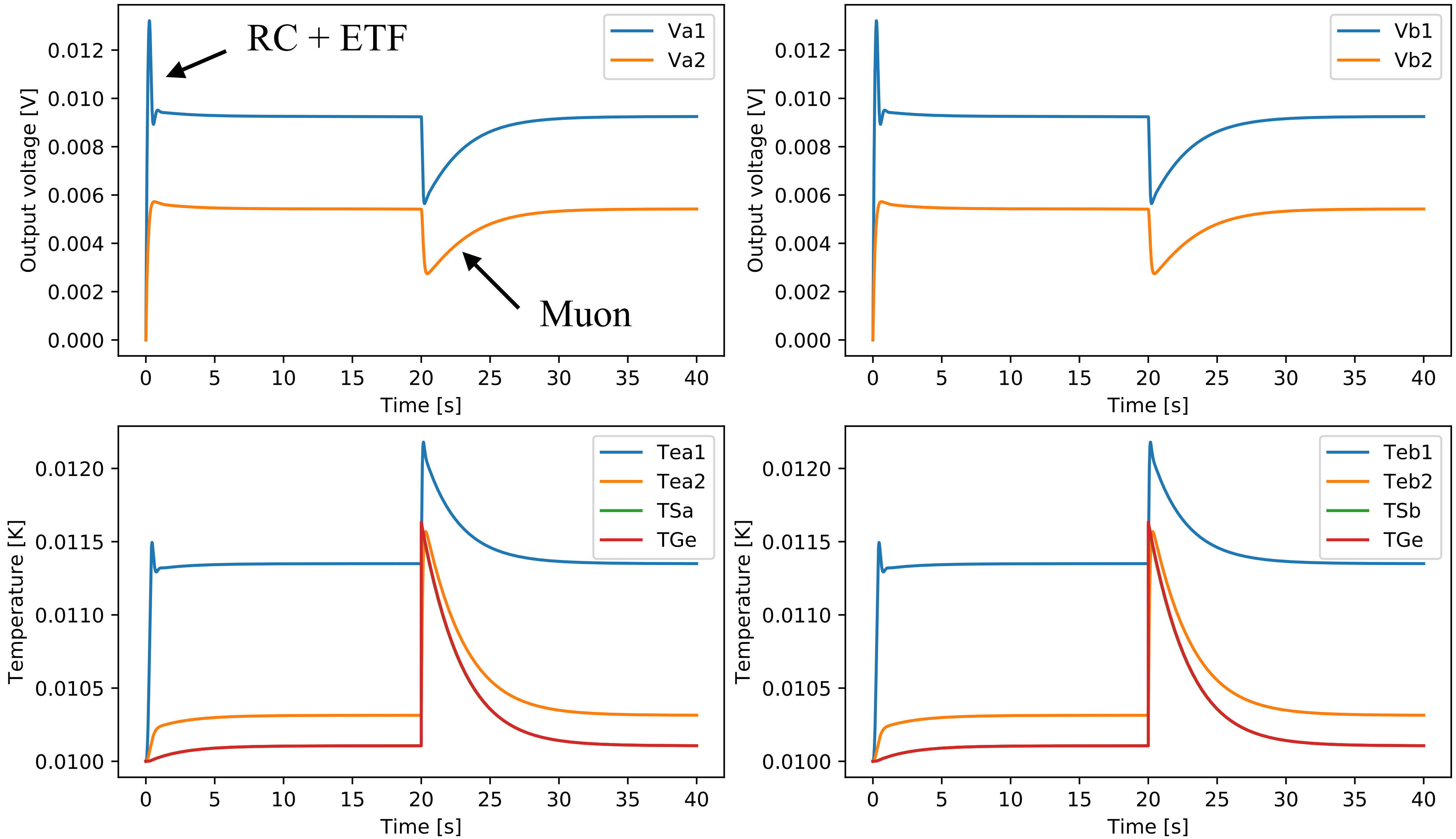

Solving the 15 dimension ODE numerically to **derive the steady states**

Also showing a 100 MeV energy deposition (muon going through) using:

Bath = 10 mK, Vbias_a1 = Vbias_b1 = 30 mV and Vbias_a2 = Vbias_b2 = 10 mV for illustration

PART III: OTHER RECENT EXAMPLES (DC POWER)

J. Billard, M. Pyle, S. Rajendran, H. Ramani, arXiv: arXiv:2208.05485

Ideal 20kg - No background

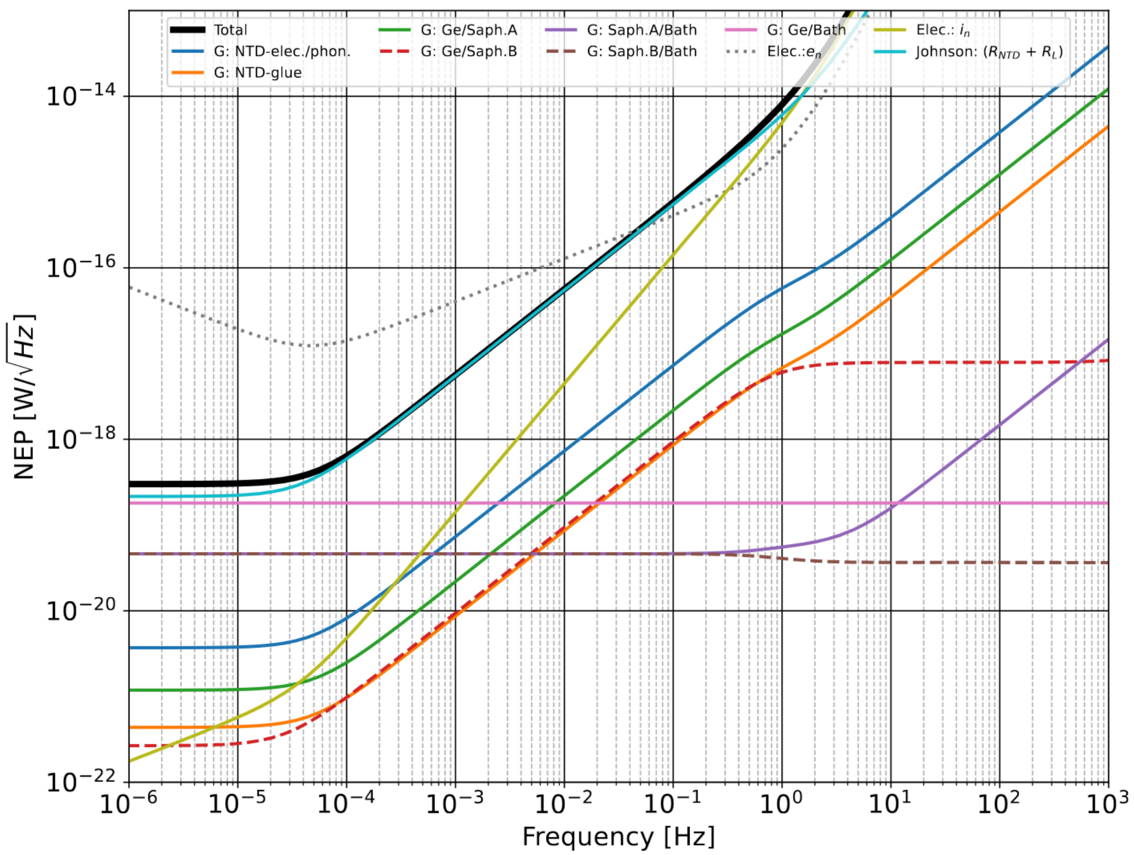

1kg - EDWIII backgrounds

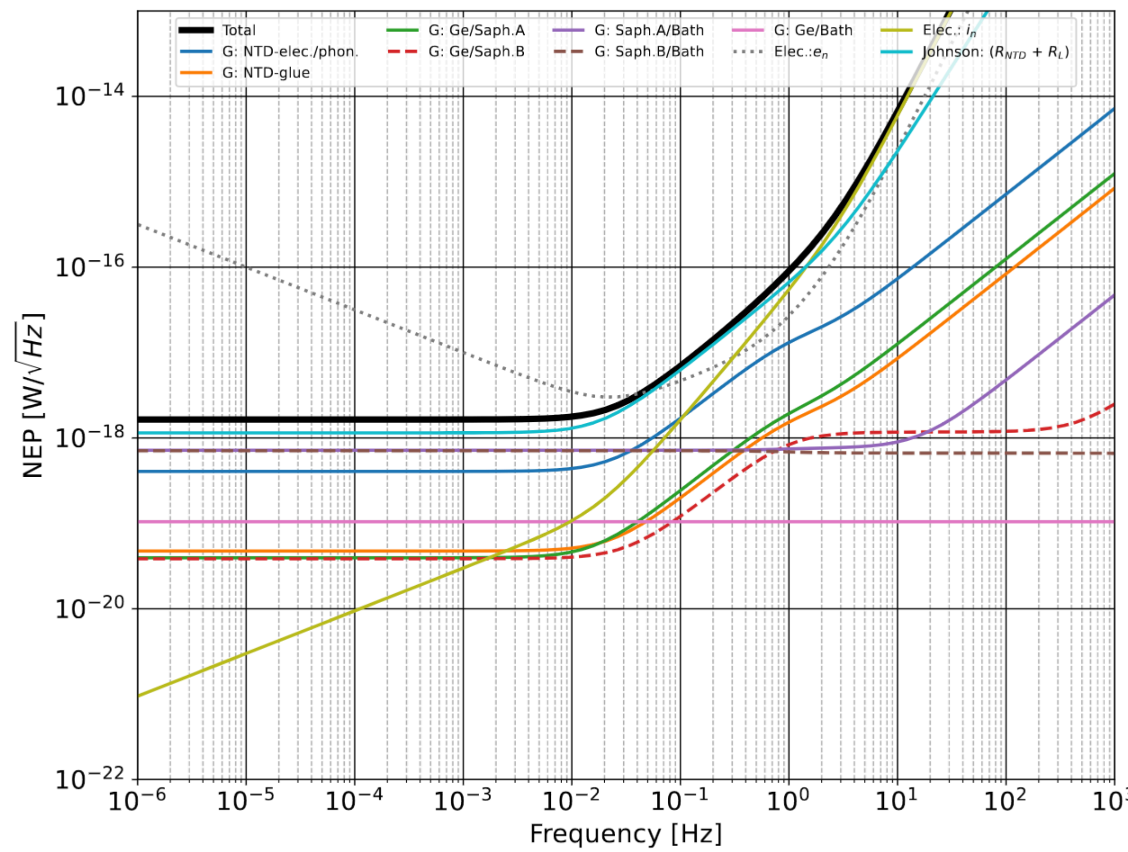

We consider two weeks of data taking leading to a DC power sensitivity (5-sigma):

- **2 x 10^{-21} W** with an ideal 20 kg detector
  Limited by the absorber-bath TFN and Johnson noise
- **1 x 10^{-20} W** with a 1 kg detector with backgrounds (1×10^{-16} W/kg)
  Limited by the sapphire phonon-phonon coupling and the Johnson noise to accommodate from the event rate

$$\sigma_{\rm DC}^2 = \int_0^{\omega_0} \frac{{\rm d}\omega}{2\pi} |{\rm NEP}(\omega)|^2 \qquad [W^2]$$

$$\downarrow$$

$$\sigma_{\rm DC} = {\rm NEP}(\omega = 0)/\sqrt{t_0}.$$

PART III: OTHER RECENT EXAMPLES (DC POWER)

J. Billard, M. Pyle, S. Rajendran, H. Ramani, arXiv: arXiv:2208.05485

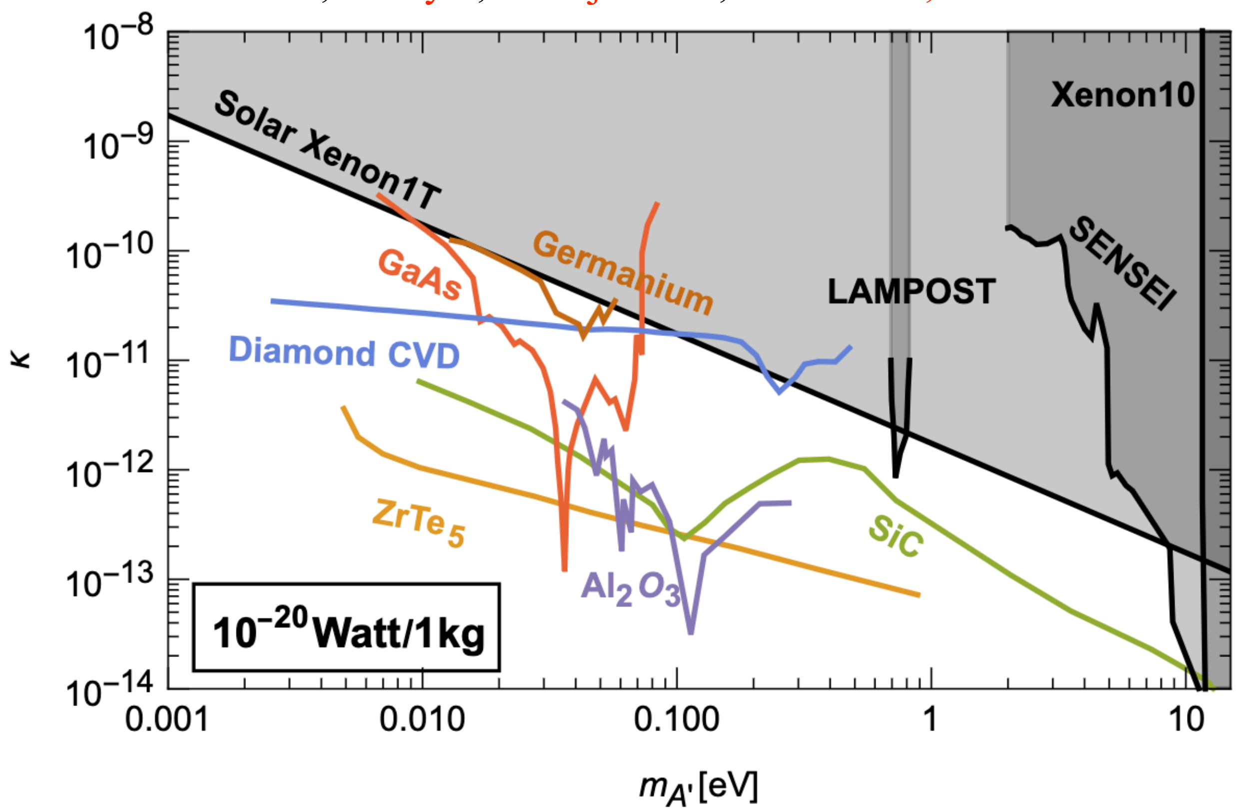

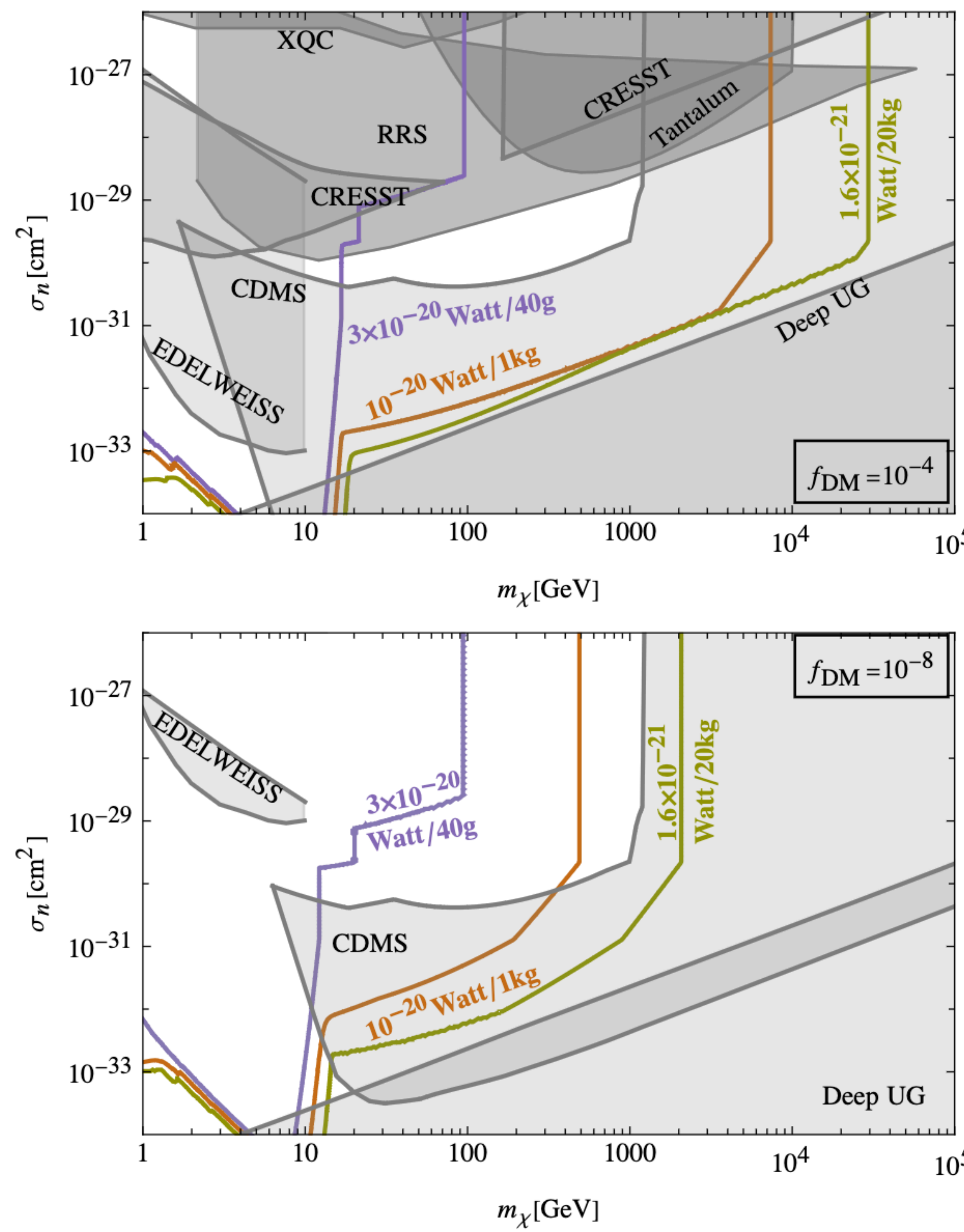

Building such a detector is very challenging as it requires precise knowledge of all the thermal conductivities of the system but it will come with significant science reach:

- Closing the gap on strongly interacting massive particle
- Extending the ALPs direct detection sensitivities to ~meV masses

CONCLUSION

Thermal modelling is a very useful tool to:

- understand our detector behaviour
- Optimize the design of our detectors and experiments with solid a priori knowledge

But one should always consider these models only as proxy to better understand their detectors

Lastly, in real life noise is usually much less easy to model: vibration, E&M pick ups, …

N. Martini PhD thesis

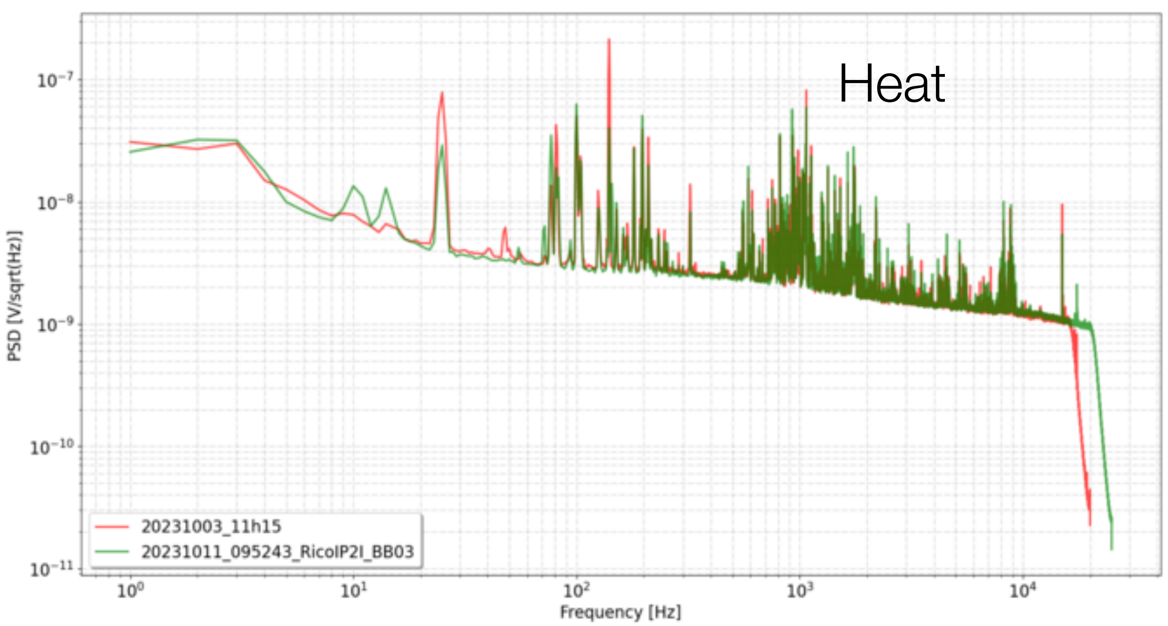

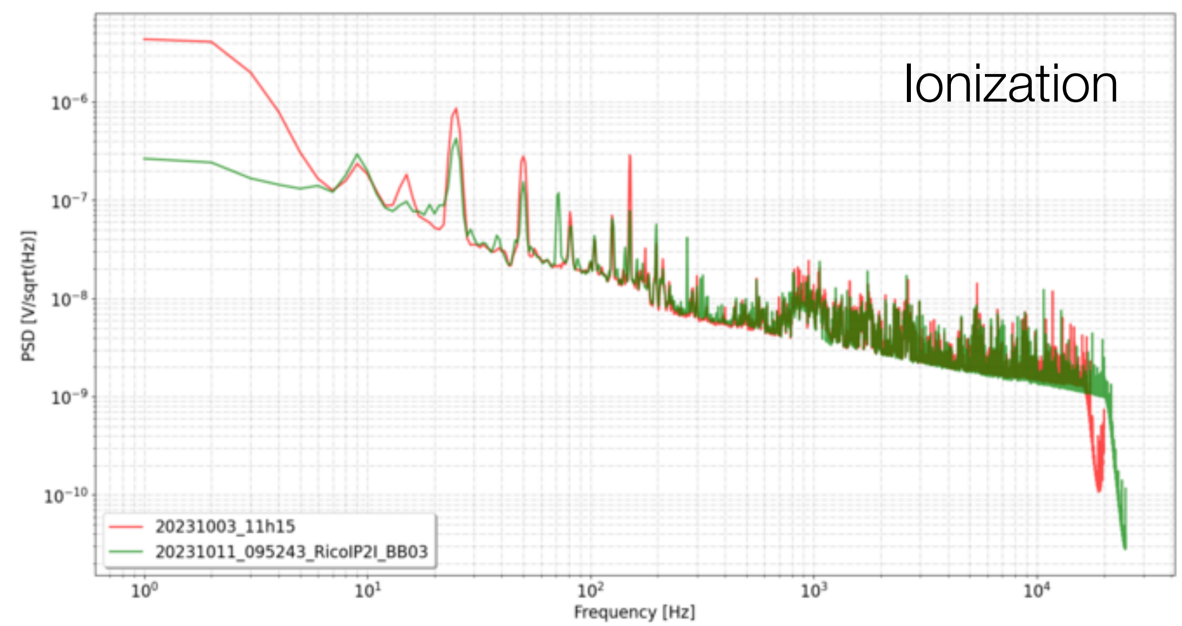

This is why data processing is key to fully optimise the output of a cryogenic detector…